Prediction and Measurement of Loading Stress on the Beechcraft King Air Tail Section

A project present to
The Faculty of the Department of Aerospace Engineering
San Jose State University

in partial fulfillment of the requirements for the degree
Master of Science in Aerospace Engineering

By

Trung- Duong H. Nguyen

May 2013

approved by

Dr. Jeanine Hunter
Faculty Advisor

The designated project titled:

PREDICTION AND MEASUREMENT OF LOADING STRESS ON THE BEECHCRAFT KING AIR TAIL SECTION

by Trung-Duong H. Nguyen

Performed and written for:

THE AEROSPACE ENGINEERING PROGRAM
SAN JOSÉ STATE UNIVERSITY

May 2013

Prof. Jeanine Hunter	Aerospace Engineering
Prof. Nikos J. Mourtos	Aerospace Engineering
Prof. Periklis Papadopoulos	Aerospace Engineering

ABSTRACT

PREDICTION AND MEASUREMENT OF LOADING STRESS ON THE BEECHCRAFT KING AIR TAIL SECTION

by Trung-Duong H. Nguyen

During flight, wings deflect up and down creating bending and torsion of stresses. These stresses must be predicted in order to design a wing with structural integrity. Wing design is a critical process. Engineers go through numerous calculations and experimental verifications of their designs prior to mass production of any aircraft. The purpose of this project is to design an experimental method to obtain stress values of an existing wing design. Modern engineers use computers to do accurate analysis on the wing (e.g. using Finite Element Method). Physical experiments with dynamically classical approaches are rare. Therefore, it is important to construct an experiment using a basic dynamic approach to bridge the gap between modern computing and classical hand calculations.

ACKNOWLEDGEMENTS

I would like to acknowledge many individuals and groups who helped me through the progress of this project. This project would not be the same without them.

First, I would like to thank all the faculty members of the Aerospace Engineering Program, consisting of Prof. Mourtos, Prof. Hunter, and Prof. Papadopoulos for supporting me and imparting knowledge and advice through the many undergraduate and graduate engineering courses I have taken at SJSU. All the knowledge and experiences gained through classroom teachers, and through advising hours after class have added up and contributed to this project.

Last, I would like to thank my colleagues and teammates; especially Gabriel Alvarez and Michelle Mojica, who have always been on my side and have supported me through many classes we have had together. My accomplishment would not be possible without these people.

Table of Contents

List of Figure

List of Table

List of Symbols

Variables

A	Total area
A_{fhi}	sectional area of leading edge curve
a_i	Area at region i
E	Young's Modulus Values of Materials
F	force
f_{hi}	parabolic function of leading curve of leading edge
$f_i(x)$	function of geometry dimension
$f_L(x)$	dimension from center of trailing edge to tip of leading edge
$f_S(x)$	dimension from center of trailing edge to center of leading edge
I_i	Moment of Inertia at region i
$I_{n.a.}$	Moment of Inertial at Neutral Axis
$L(x)$	height of the parabolic-shape leading edge
m_i	mass of component i
M_i	Bending moment at region i
P	Load
q_i	Shear at section i
T_i	Overall width
t_i	thickness of region i
V_i	Shear at region i
w_i	width of region i
X_i	x component of centroid location in Universal Coordinate System
X_{ci}	x component of centroid location in Centroid coordinate system
Y_i	y component of centroid location in Universal Coordinate System
Y_{ci}	y component of centroid location in Centroid coordinate system

Greek Symbols

σ	general stress value
σ_{th}	theoretical stress value
σ_{exp}	experimental stress value
ε_{exp}	strain value from strain gage
Σ	summation
$\int$	intergral

Miscellaneous Notations

□	constant
□	see above
↓	see below

1.0 INTRODUCTION

There are many ways to estimate the aerodynamic loads on an airfoil in flight. For this project, we will apply a physical load onto the tail section to simulate load. The idea here is to develop and define a new technique to predict bending stress on an airfoil. Knowing the aerodynamic loading, we can predict wing deflection and structural strain during flight.

A Beech 200 (King Air) tail section will be considered to be a wing and used as the experimental setup for this project. This tail section will be divided into small spanwise sections and an incremental lift force applied to the center of gravity of each section. Strain gages will be applied to the tail section, and strain will be measured experimentally and then compared with the predicted values.

This analysis will compare the results of the theoretical and experimental methods. Depending on the resulting error, further analysis or extensive revision of the theoretical method may be required. Also, other sources of error from approximations and assumptions will be evaluated to ensure consistent result.

1.1 MOTIVATION

In the past years, numerous of experimental works have been done to verify the loading stress on the wing. However, none of them tackle the experiment with classical approaches from the perspective of dynamics and statics (analyze characteristics of the material based on the cross section profile). That type of approach was only used during development but is rarely seen during testing.

2.0 Objectives

- Construct a device to simulate load on the tail section of a Beech King Air
- Use the obtained strain values from the device. Calculate strain/stress at multiple points on the tail analytically
- Apply strain gauges at certain points on the tail. Compare the reading from the strain gauge with the calculated value
- Use obtained values to determine shear flow and shear stress
- For each cross section, determine position of shear flow
- Simplify the process and create lab experiment for AE114

3.0 Literature Review

Most wings share similar characteristics to create lift and induce maneuvers during flights. It is important to know some basic background on the experiments have been done in the past, how they did it, and what type of wing is given for the project.

3.1 Background

To develop an experimental method of measuring stress on a wing design, we're given a tail section from an aircraft Beech King Air model, designed and developed by Hawker Beechcraft Corporation, manufactured by Collins. The tail section has been salvaged and obtained from the SJSU Aviation Department with much of the effort from Professor Hunter at SJSU with the purpose of giving SJSU Aerospace students some hands-on experience with real life applications. Through numerous researches for detail specifications of its design, we learned that Hawker Beechcraft Corporation does not release its blue print design without a minimum fee of $200 plus $100 per hour research for its engineers to export their drawings. Without the blueprint, we won't be able to replicate the exact dimensions of this tail section design; however, we can still manually take measurements with acceptable errors.

There are numerous methods in testing loading stress on a wing in the past. Most of them are confidential documents of private corporations and governments. Therefore, resources on these methods are very limited. This project is to develop a new method to measure and analyze stress on a wing. So what we need are benchmarks from similar designs to validate our values and basic knowledge from statics and dynamics.

3.2 What has been done in the past:

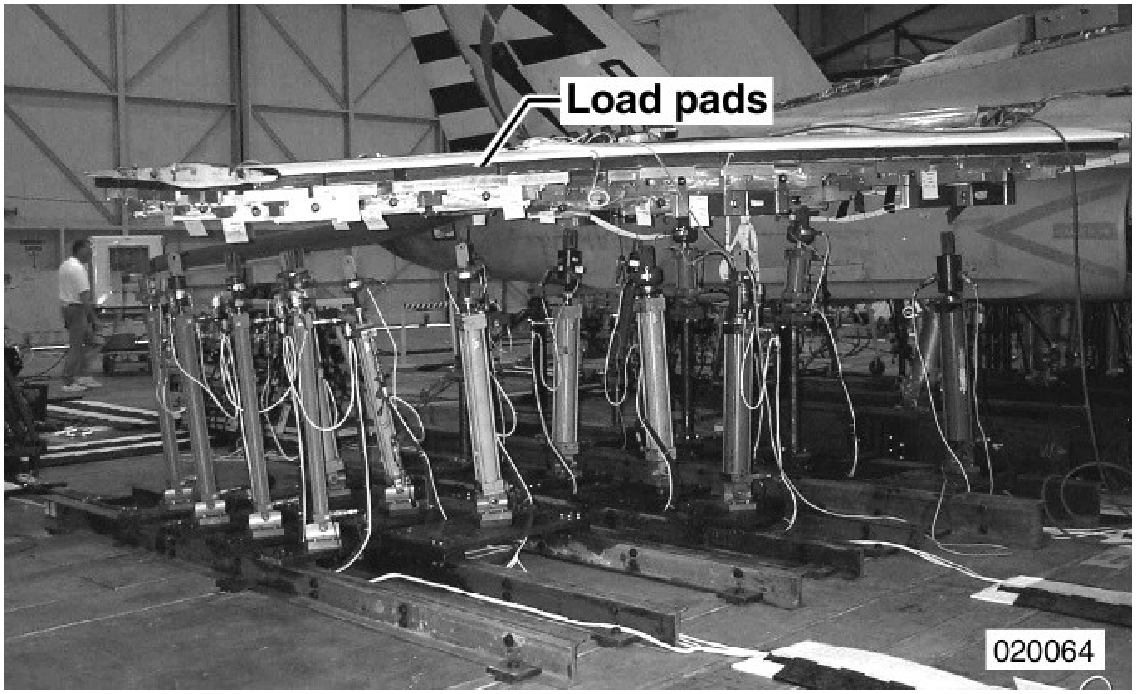

Figure 3-1: NASA's strain gage loads calibration test set up on the AAW Wing. (Crawford, 2002)

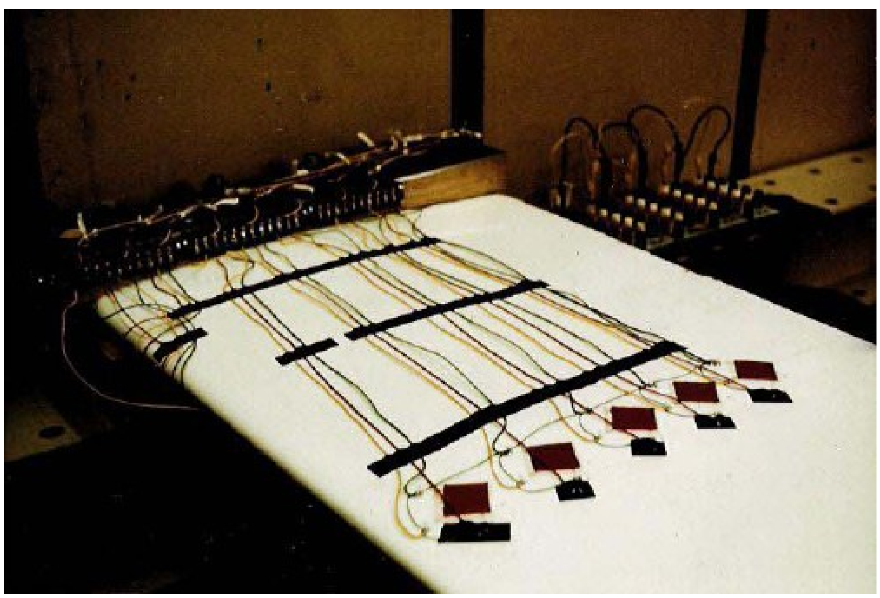

Figure 3-2: Applying Strain Gage (Kriz, 1973)

Figure 3-3: Applying Sandbags

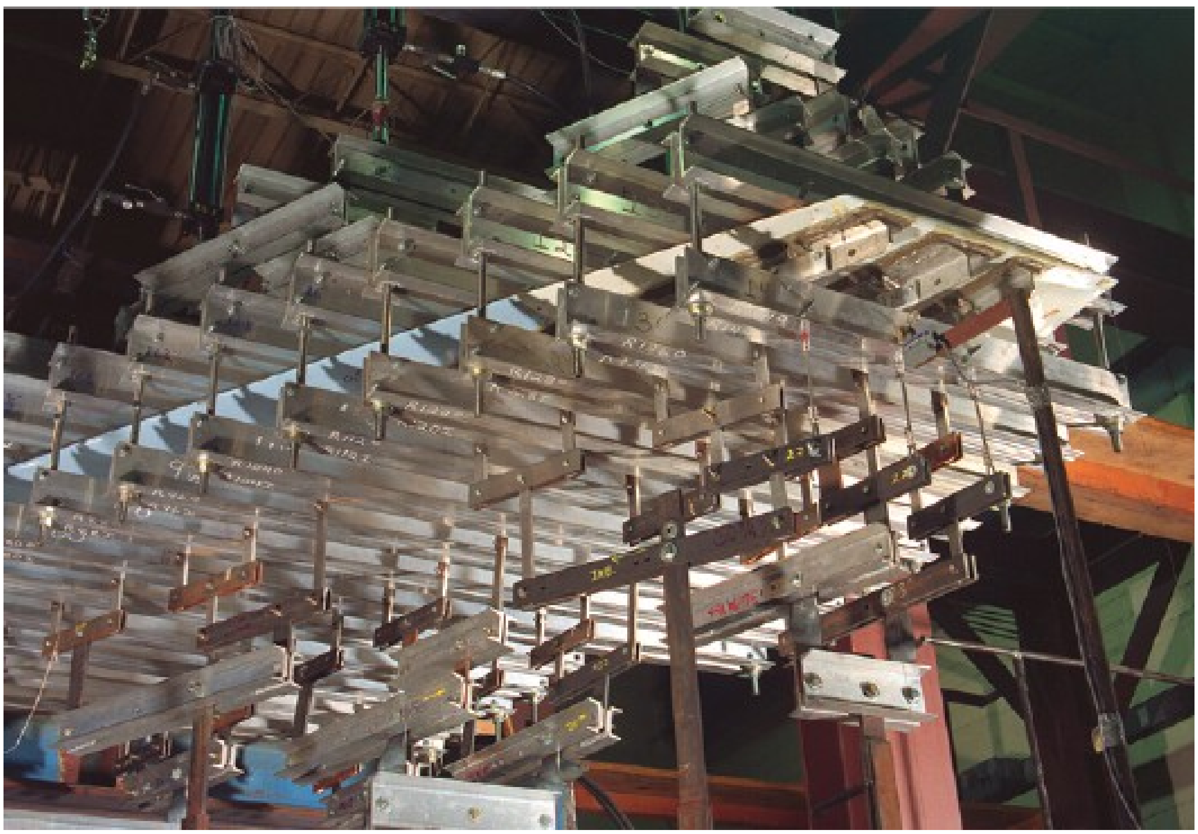

Figure 3-4: Distributed Wing Load Test (Southwest Research 2010)

Figure 3-5: Lift Simulation (Juraeka & Jekacek, 2000)

All of these tests applied direct forces on the wing. Upon applying the strain gages along the wing, we can easily read the strain values recorded as we physically apply the forces on it. In 2002, NASA conducted a loading test on an F/A-18 fighter jet. The loads were measured using an array of strain gages on structural members of the wing. This test consists of inputs for loading, and outputs from the strain gage readings. The data was then used to develop equations for shear, bending moment, and torque loads. Hydraulic cylinders were used to simulate lift by pushing upward. The load pads and loading hardware were developed to be able to apply loads directly into the structure; therefore, the skin of the wing was cut out. At the loading mounts, panels were fabricated into the mountings to provide same structural rigidity as when the skin structure was still there.

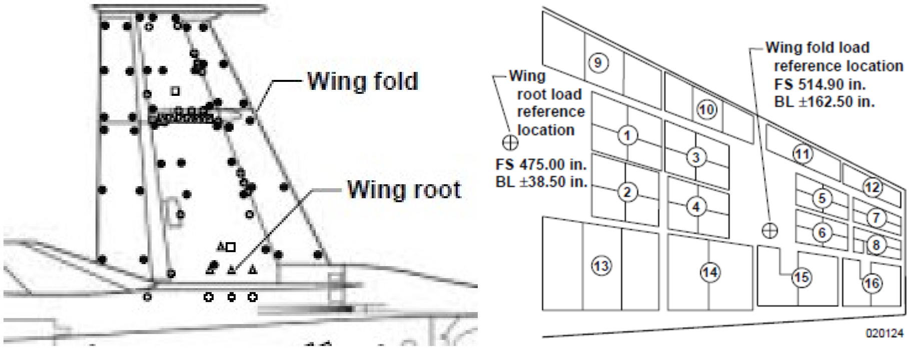

Figure 3-6: Locations of the Gages (Lokos, Olney, Chen, & Crawford, 2002)

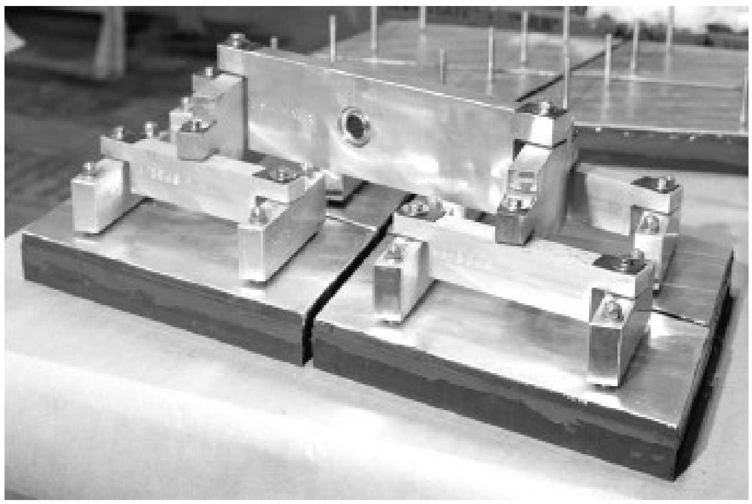

Figure 3-7: Loading Mounts (Lokos, Olney, Chen, & Crawford, 2002)

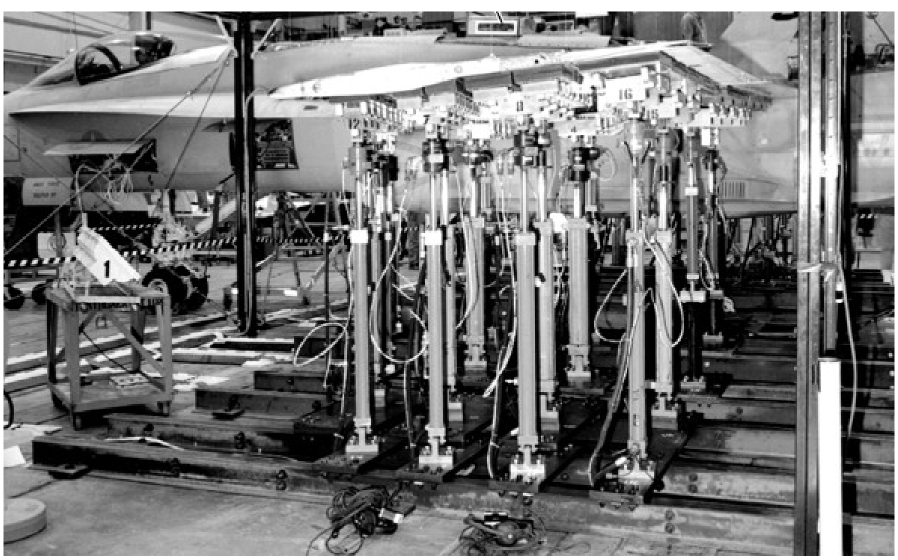

Figure 3-8: Hydraulic Cylinders (Lokos, Olney, Chen, & Crawford, 2002)

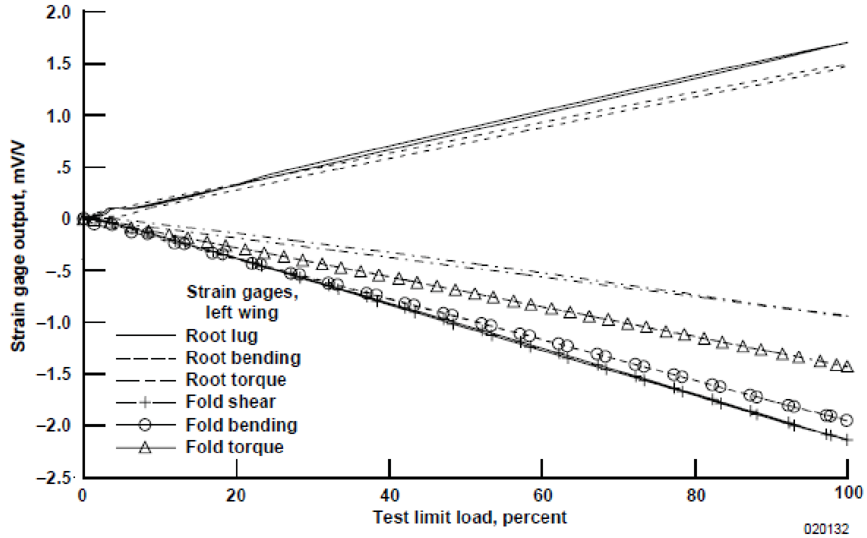

Figure 3-9: Strain-gage output at control-surface hinges. (Lokos, Olney, Chen, & Crawford, 2002)

3.3 WHAT HAS BEEN MISSING

Past research and experiments lack technical data requisite in determining on how to physically calculate and measure the strain and stress on a given airfoil without the blueprints. Nonetheless, none of them approached the problem with the classical method from the standpoint of Statics and Dynamics. All of them started the experiment from a conceptual basis that was prepared based on the prototype.

3.4 CURRENT PROBLEM

The tail wing was designed with the same technology as the main wing, but with a smaller scale in terms of performance. From this point of view, we'll assume that our numbers and calculation values will be in a small scale that is comparable to the main wing. The wing is approximately 7 feet long, 2 feet wide at the root, and 1.5 feet wide at the tip. Even though, it is placed at the tail for stability which does not handle most of the aircraft's mass, we'll assume it is fully operational to generate lift. Upon obtaining the tail section, all we know is that the tail belongs to a Beech King Air model. Hawker Beechcraft created 5 models of King Air series: Beech 100 King Air, Beech 200 Super King Air (C-12), Beech 300 Super King Air, Beech 350 Super King Air, and Beech 90 King Air (C-6) (Lednicer, 2010). Lucky for us, all of these models share the same wing configuration. The wing root is NACA 23018, and the wing tip is NACA 23012 (Lednicer, 2010).

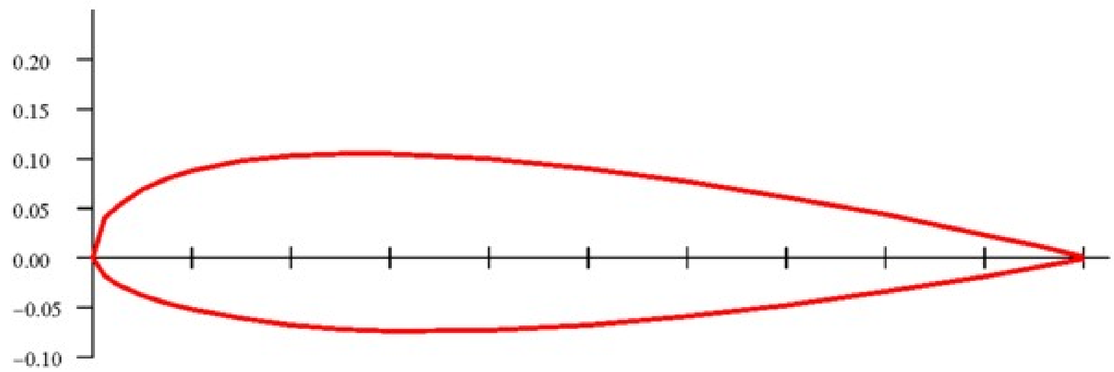

Figure 3-10: Wing Root NACA 23018 (Airfoil Investigation Database, 2012)

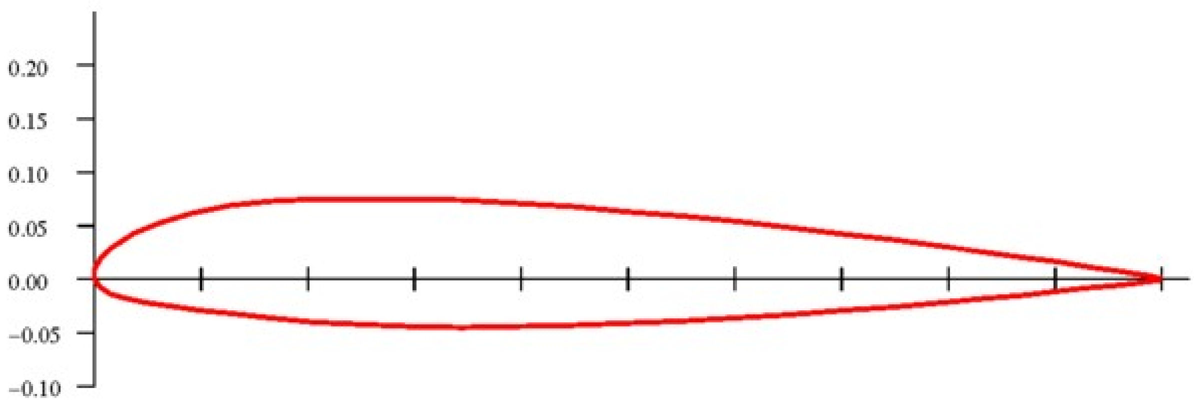

Figure 3-11: Wing Tip NACA 23012 (Airfoil Investigation Database, 2012)

As we now observe, the cross-section of the airfoil is almost symmetrical. Upon closer inspection of the cross-section of the wing, we observed the stringers and other components attached along the wing to create rigidity for the structure.

Figure 3-12: Beech King Air Tail Section

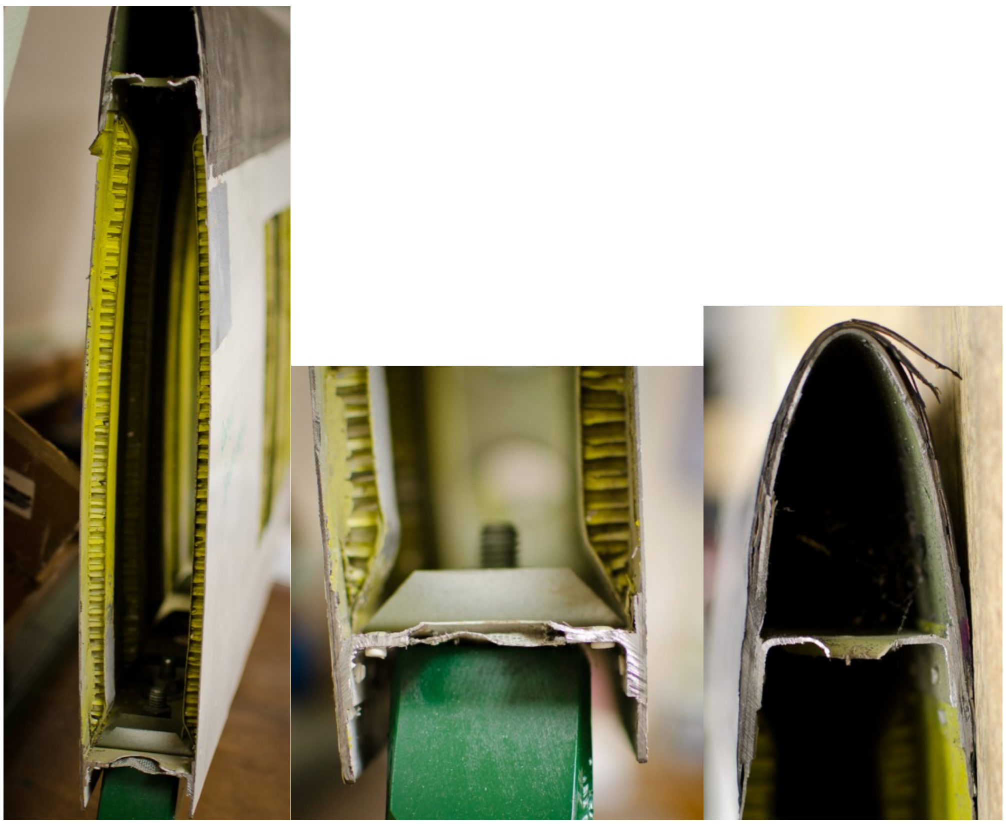

Figure 3-13: (a) (b) (c) Observed Cross Section of the Tail Section

Figure 3-14: Stringers along the wing and the Backing Support with Cutout Holes

As illustrated in Figure 13 & 14, stringers and beams are attached along the wing span to increase rigidity and reduce torsion during flexes. Thanks to the cutout of the extra spare wing, we can measure and obtain dimensions of the cross section manually.

4.0 Preliminary Calculations

The tail section consists of stringers, beams, and the skin. Each of these components plays a major role in determining the characteristics of the airfoil. To accurately analyze and understand the strain and stress of the airfoil, we will use the classical approach from Fundamental Beam Theory. The moment of inertia is one property of the structure which deals with the entire mass of the cross section with a designated centroid. From the location of the centroid and the moment of inertia of the cross section, the bending stress can be determined as well.

The airfoil gets thinner at the tip, so the cross sections have gradually varied dimensions rather than uniformity throughout the airfoil. This is where we will analyze and experiment to see whether the moment of inertia changes linearly or not along the wingspan.

Once the moment of inertia for cross sections along the wingspan is calculated, it is possible to obtain the bending stress and strain. That will lead us to finding the deflection of the wing. The stages of calculations are as followings:

1. moment of inertia (property for each cross section)
2. moment of inertia relation along the wingspan (determine if it’s linear or not)
3. bending stress/strain
4. shear flow
5. deflection

4.1 Classical Approach

A theoretical calculation is desired in order to compare experimental results with respect to a parameter of interest. Upon our discovery of the structure’s cross-section, we can take measurements to obtain dimensional values. Once the values are obtained, we’ll calculate the stress on the entire wing in the following order: moments of inertia, bending stress/strain relation along the wingspan, shear flow, and deflection. Below is the diagram of the generalized cross sections of the wing with only the main stringers.

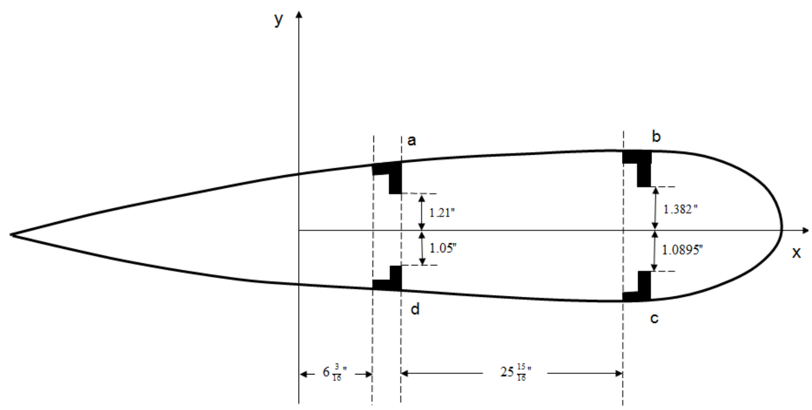

Figure 4-1: Generalized Placement of the Stringers inside the wing

With the dimension values, the moment of inertia can be calculated via

$\acute{x}=\sum \frac{x_i A_i}{A}$ in which $\acute{x}$ is the moment of inertia about the x-axis (the direction of torsion resulted from wing deflection), x_i is the distance of the x-component from the centroid, and A_i is the area of each component (cross sectional area of the stringers). From that, we should have the bending moment for that specific cross-section. This method will be applied for 26 evenly-spaced cross-sections along the entire wingspan. (Hibbeller, 2007)

With all data recorded, the entire wing can almost be treated as a cantilever beam with a defined bending moment at each cross-section.

4.2 Cross Section Calculation

Cross section calculation is the very first step to get all dimensions of the cross section before calculating the moment of Inertia and Bending Moment. The very first step to analyze the structure of the tail section is to break down the entire airfoil into small components. Each component will be identified and labeled in order. The whole tail section has multiple components which are divided into 14 regions (not counting the thin skin connecting between leading edge and trailing edge):

1. Generally, there are 4 main stringers (Figure 4-1) placed along the wingspan. For our practical purpose, these 4 stringers are divided into 8 regions to make calculation easy: Region 1, 2, 3, 4, 6, 7, 10, and 11. (Labeled in Figure 4-2, Figure 4-3, and Figure 4-4)
2. Region 5 is the back support for stringers of Region 1, 2, 3, and 4. (Figure 4-3)
3. Region 8 and 9 is also the back support for stringer of Region 6, 7, 10, and 11. This back support has cut out holes at every 4 in along the wingspan to save weight. Hence, Region 8 only exists at every other cross-section. (Figure 3-14 and Figure 4-4)
4. Region 12, 13, and 14 are the leading edge surfaces (Figure 4-4). We divide this section into 3 regions to make our calculation simple and effective. (See Figure 4-5 and Section 4.2.3)

The cross section of the wing is simplified in Figure 4-2:

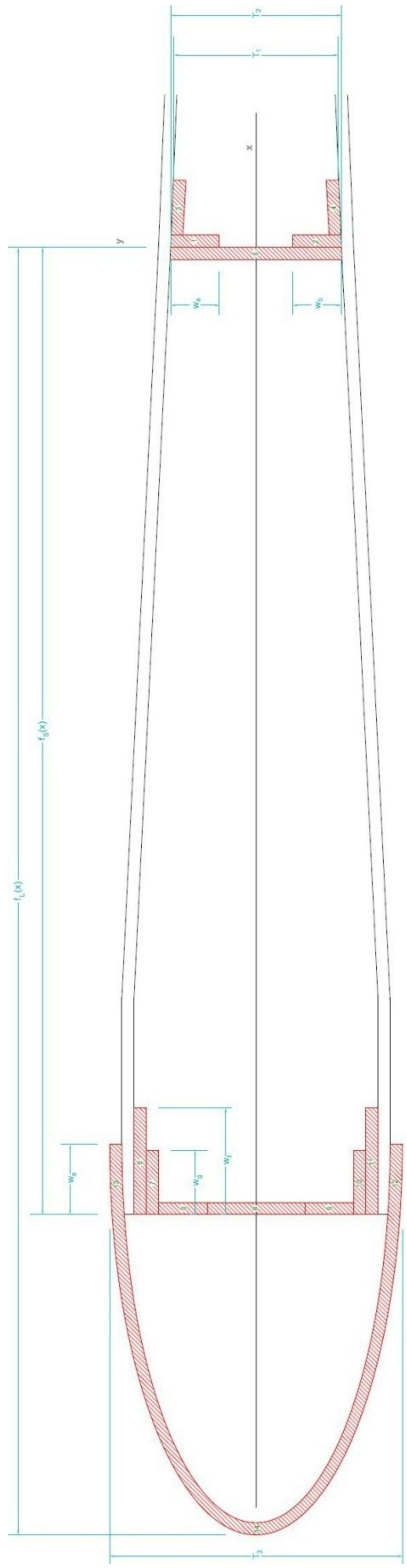

Figure 4-2: Leading Edge with length $f_S(x)$. Not to scale

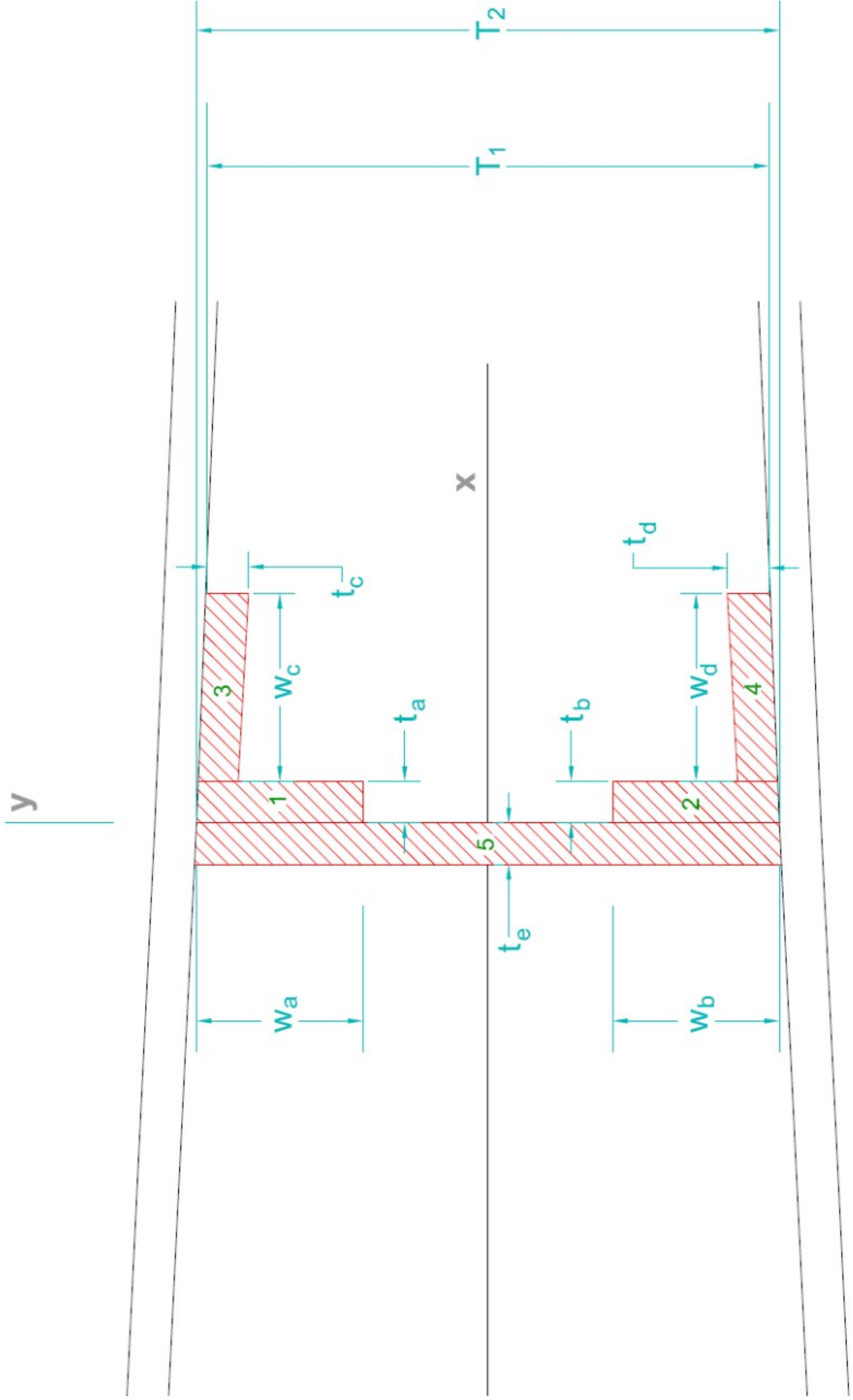

Figure 4-3: Trailing Edge Cross Section. Not to scale

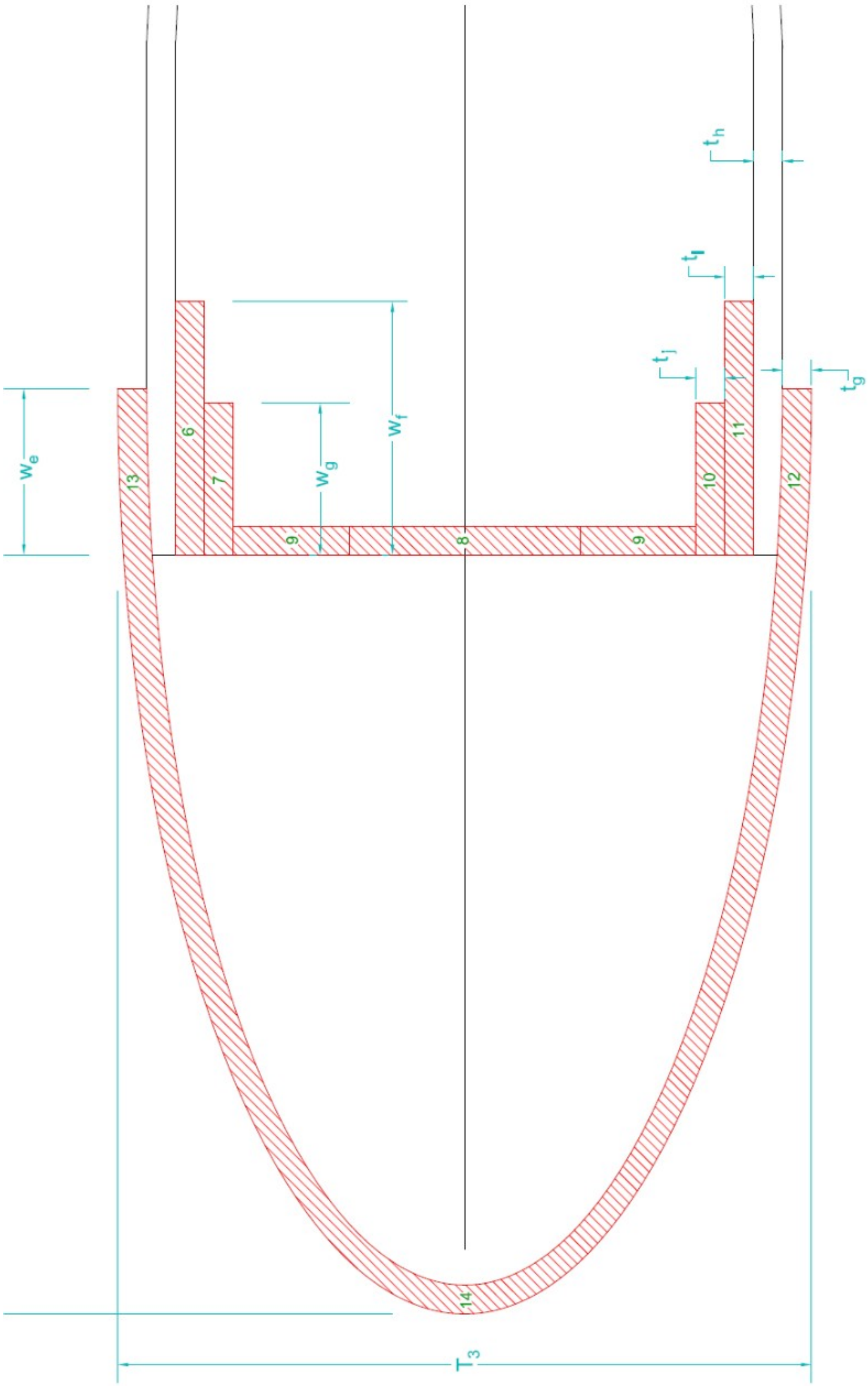

Figure 4-4: Details of Leading Edge Cross Section. Not to scale

From these diagrams, we should be able to calculate each individual's components (see Appendix A):

1. Area (a_i)
2. Center of Mass of each Component (x_i, y_i)
3. Center of Mass in Centroid Coordinate System (x_{ci}, y_{ci})

Before this can be performed accurate measurements must be made to obtain numerical values by calculation. (See Appendix B for measurement data)

4.2.1 Variables that needs to be measured with a precision micrometer:

Thickness of materials: t_a, t_b, t_c, t_d, t_e, t_f, t_g, t_h, t_i, and t_j

Width of each elements in a cross-section: w_a, w_b, w_c, w_d, w_e, w_f, and w_g

Airfoil thickness at the center truss of trailing edge: T_2 and T_1

Airfoil thickness at the center truss of leading edge: T_3

Distance from center of trailing edge to center of leading edge: $f_S(i)$ with respect to i^{th} cross sectional area.

Distance from center of trailing edge to the tip of leading edge: $f_L(i)$ with respect to i^{th} cross sectional area.

4.2.2 Properties of each member within a cross-section area

Area for each member within a cross-section area will be $a_i = w_i \cdot t_i$

Eq. 1

Center of mass for each member will be defined as (x_i, y_i)

Centroid of area A under $f(x)$, x component $\acute{x} = \frac{1}{A}\int_a^b x \cdot f(x)\,dx$ Eq. 2

Centroid of area A under $f(x)$, y component $\acute{y}=\frac{1}{A}\int_a^b \frac{1}{2}[f(x)]^2 dx$ Eq. 3

Centroid of area A between $f(x)$ and $g(x)$ region, $\acute{x}$

$$\acute{x}=\frac{1}{A}\int_a^b x[f(x)-g(x)]dx$$ Eq. 4

Centroid of area A between $f(x)$ and $g(x)$ region, $\acute{y}$

$$\acute{y}=\frac{1}{A}\int_a^b \frac{1}{2}\{[f(x)]^2-[g(x)]^2\}dx$$ Eq. 5

4.2.3 Leading Edge's tip Preliminary Calculations

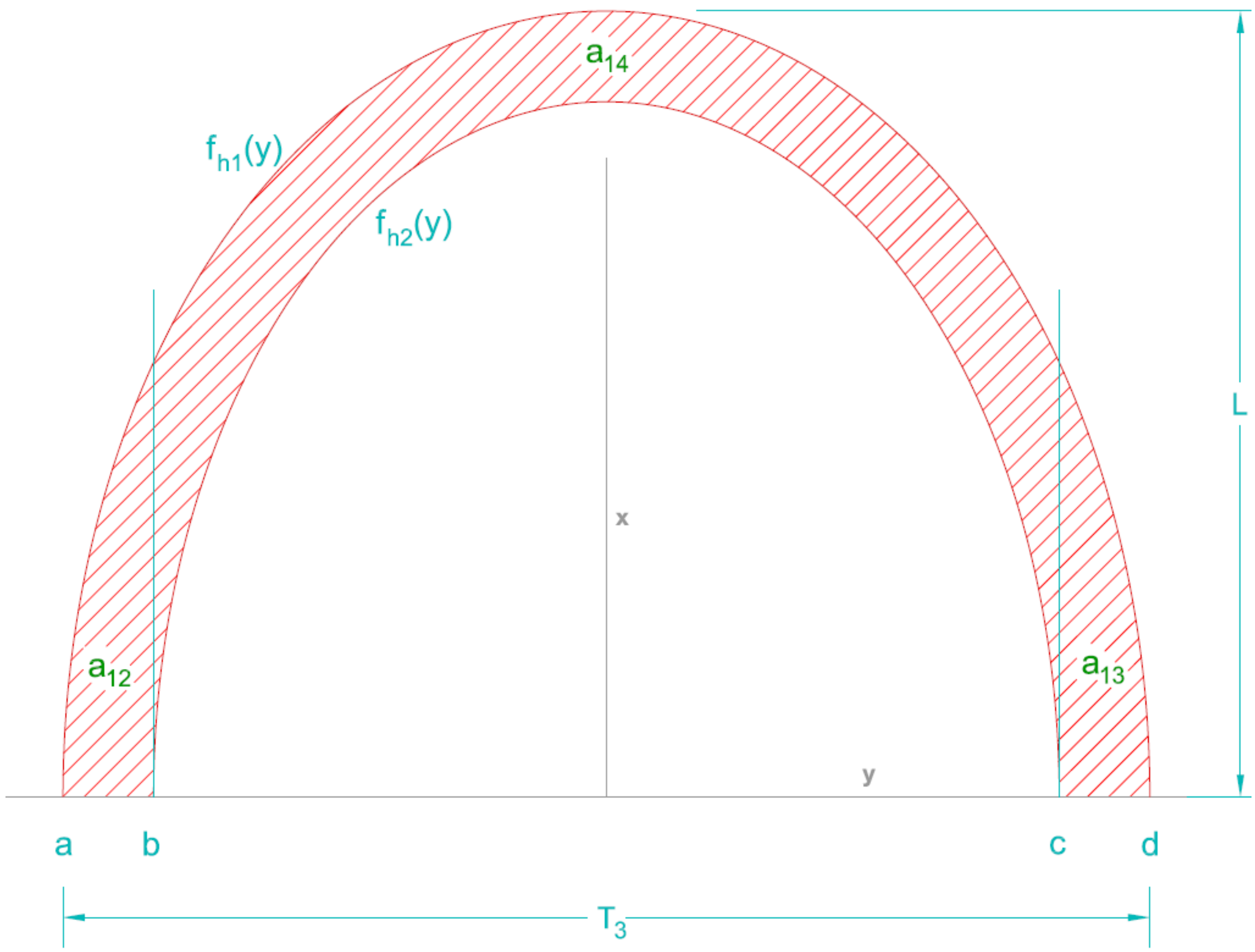

Figure 4-5: Parabolic shape to approximate Leading Tip. Not to scale

The best approximation for the shape of the Leading Edge's Cross Section is modeled with a Parabolic Equation. From basic algebra operation, the equation for any parabolic curve with the vertex (0, L) and zeros at (-0.5T, 0) and (0.5T, 0) is

$$f(x)=\frac{-4L}{T^2}\cdot x^2+L \qquad \text{Eq. 6}$$

Height of the Tip $L(i)=f_L(i)-f_s(i)-w_e$ Eq. 7

Outer Parabolic Curve for the tip $f_{h1}(y)=\frac{-4L}{T_3^2}y^2+L$ Eq. 8

Inner Parabolic Curve for the tip (minus by thickness t_g)

$$f_{h2}(y)=\frac{-4(L-t_g)}{(T_3-2t_g)^2}y^2+(L-t_g)$$ Eq. 9

<u>Area under curve $f_{hi}(x)$:</u>

$$A_{fh1} = \int_a^b f_{h1}(y)\,dy$$ Eq. 10

$$A_{fh1} = \int_a^b \left(\frac{-4L}{T_3^2} y^2 + L \right) dy$$ Eq. 11

$$A_{fh1} = \left[\frac{-4L}{3T_3^2} y^3 + Ly \right]_a^b$$

Eq. 12

Similarly, A_{fh2} has the same structure as Eq.11, but with a decrease in thickness t_g all around:

$$A_{fh2} = \left[\frac{-4(L-t_g)}{3(T_3-2t_g)^2} y^3 + (L-t_g)\,y \right]_a^b$$

Eq. 13

Area of member a_{14} should be the difference between A_{fh1} and A_{fh2}

$$a_{14} = A_{fh1} - A_{fh2}$$ Eq. 14

Define position a, b, c, and d from Figure 4-5

$a = -d = 0.5 \cdot T_3$ Eq. 15

$b = -c = 0.5 \cdot T_3 - t_g$

Eq. 16

Centroid for a_{12} and a_{13}

$\acute{x}$ $$x'_{12} = x'_{13} = \frac{1}{A_{fh1}} \int_c^d 0.5 \left[f_{h1}(y) \right]^2 dy$$ Eq.17

$$x'_{12} = x'_{13} = \frac{1}{A_{fh1}} \int_c^d 0.5 \left[\frac{-4L}{T_3^2} y^2 + L \right]^2 dy$$ Eq. 18

$$x'_{12} = x'_{13} = \frac{1}{2A_{fh1}} \int_c^d \left[\frac{16L^2}{T_3^4} y^4 - \frac{8L^2}{T_3^2} y^2 + L^2 \right] dy$$

Eq. 19

$$x'_{12} = x'_{13} = \frac{1}{2A_{fh1}} \left[\frac{16L^2}{5T_3^4} y^5 - \frac{8L^2}{3T_3^2} y^3 + L^2 y \right]_c^d$$

Eq. 20

$\acute{y}$ $$y'_{12} = y'_{13} = \frac{1}{A_{fh1}} \int_c^d y \cdot f_{h1}(y) dy$$ Eq. 21

$$y'_{12} = y'_{13} = \frac{1}{A_{fh1}} \int_c^d y \cdot \left[\frac{-4L}{T_3^2} y^2 + L \right] dy$$

Eq. 22

$$y'_{12} = y'_{13} = \frac{1}{A_{fh1}} \left[\frac{-L}{T_3^2} y^4 + \frac{L}{2} y^2 \right]_c^d$$ Eq. 23

Centroid for a_{14}

$\acute{x}$ $$x'_{14}=\frac{1}{2A}\int_b^c\left\{\left[f_{h1}(y)\right]^2-\left[f_{h2}(y)\right]^2\right\}dy$$

Eq. 24

$$x'_{14}=\frac{1}{2\left(A_{fh1}-A_{fh2}\right)}\int_b^c\left\{\left[\frac{-4L}{T_3^2}y^2+L\right]^2-\left[\frac{-4\left(L-t_g\right)}{\left(T_3-2t_g\right)^2}y^2+\left(L-t_g\right)\right]^2\right\}dy$$

Eq. 25

$$x'_{14}=\frac{1}{2\left(A_{fh1}-A_{fh2}\right)}\int_b^c\left\{\begin{matrix}\left[\frac{16L^2}{T_3^4}y^4-\frac{8L^2}{T_3^2}y^2+L^2\right]\\-\left[\frac{16\left(L-t_g\right)^2}{\left(T_3-2t_g\right)^4}y^4-\frac{8\left(L-t_g\right)^2}{\left(T_3-2t_g\right)^2}y^2+\left(L-t_g\right)^2\right]\end{matrix}\right\}dy$$

Eq. 26

$$x'_{14}=\frac{1}{2\left(A_{fh1}-A_{fh2}\right)}\left[\begin{matrix}\left[\frac{16L^2}{5T_3^4}y^5-\frac{8L^2}{3T_3^2}y^3+L^2y\right]\\-\left[\frac{16\left(L-t_g\right)^2}{5\left(T_3-2t_g\right)^4}y^5-\frac{8\left(L-t_g\right)^2}{3\left(T_3-2t_g\right)^2}y^3+\left(L-t_g\right)^2y\right]\end{matrix}\right]_b^c$$

Eq. 27

$\acute{y}$ $$y'_{14}=0$$

Eq. 28

4.3 Cross Section Properties

Each individual member of the cross section area has properties to be evaluated.

a_i = area of member i at coordinate (x_i, y_i)

A = total area = Σ a_i

Coordinate of Centroid: $\acute{X} = \sum_{1}^{i} \frac{x_i \cdot a_i}{A}$ $\acute{Y} = \sum_{1}^{i} \frac{y_i \cdot a_i}{A}$

Moment of Inertia: $I_{\acute{X}} = \sum_{1}^{i} a_i \cdot (y_{ci})^2$ $I_{\acute{Y}} = \sum_{1}^{i} a_i \cdot (x_{ci})^2$ $I_{\acute{X}\acute{Y}} = \sum_{1}^{i} a_i \cdot x_i \cdot y_i$

Stress: $\sigma = \frac{M_y}{I_{n.a.}}$

(Hibbeller, R.C.)

Since all Regions are rectangular shaped (except region 12, 13 and 14), their individual centroid should be right in the middle of their bodies.

For region 12, 13, and 14, their centroid should follow Eq.17 to Eq. 28.

These Equations will be incorporated into excel to generate all $\acute{X}, \acute{Y}, I_{\acute{X}}$ and $I_{\acute{Y}}$.

See Table 4-1 for results.

4.4 Results: Theoretical Centroid and Moment of Inertia

i	Distance from tip (in)	$\acute{X}$ (in)	$\acute{Y}$ (in)	$I_{\acute{X}}$ (in^4) no skin	$I_{\acute{Y}}$ (in^4) no skin	$I_{\acute{X}}$ (in^4) with skin	$I_{\acute{Y}}$ (in^4) with skin
1	15.375	-10.07531453	-0.01043	0.214819	49.9921	0.211998	51.84494
2	18.375	-9.959288723	-0.01338	0.2722	57.31588	0.269274	58.829
3	21.375	-10.99045339	-0.00972	0.31264	54.94158	0.310228	57.74353
4	24.375	-10.47471023	-0.02146	0.344196	66.62019	0.339662	68.41212
5	27.375	-11.31242985	-0.02445	0.414719	66.00381	0.409335	68.87453
6	30.375	-10.59729437	-0.03079	0.455742	81.16514	0.4485	82.71008
7	33.375	-11.25666786	-0.01118	0.505746	82.69948	0.501913	84.98498
8	36.375	-10.94377212	0.000707	0.548007	95.056	0.547167	96.64663
9	39.375	-11.83666681	-0.03316	0.596601	94.02446	0.586993	96.79064
10	42.375	-11.24707087	-0.00401	0.639672	111.1341	0.637453	112.7072
11	45.375	-12.25762118	-0.03171	0.695727	108.55	0.684828	111.5447
12	48.375	-8.500050888	0.001401	1.590863	173.4229	1.590028	173.6676
13	51.375	-8.981312954	-0.00664	1.742319	180.4738	1.738364	180.5821

14	54.375	-11.16892264	0.007194	1.126037	159.6604	1.127403	160.3577
15	57.375	-10.7396064	0.003683	1.380379	180.3361	1.380556	180.5686
16	60.375	-11.45314301	0.101112	1.879298	183.6589	1.899323	184.3021
17	63.375	-10.57496566	-0.01411	1.826236	213.7266	1.818942	213.7562
18	66.375	-10.46252416	-0.02337	2.100238	232.4579	2.08862	232.4579
19	69.375	-10.23964054	0.001115	2.469052	254.3751	2.468343	254.4392
20	72.375	-10.09296243	0.001311	2.798161	275.9779	2.79759	276.1874
21	75.375	-10.0314954	-0.01091	3.142296	297.05	3.135725	297.4252
22	78.375	-9.78937	-0.0209	3.595492	323.1099	3.583699	323.8859
23	81.375	-9.704206368	0.004227	3.873856	347.0379	3.875088	348.1507
24	84.375	-9.695411654	-0.00559	4.238057	370.394	4.234084	371.7941
25	87.375	-9.5722674	-0.01674	4.75558	397.5939	4.745451	399.51
26	90.375	-9.712427095	-0.014	5.061324	419.4749	5.052492	421.4985

Table 4-1: Universal Centroid of Mass & Total Moment of Inertia

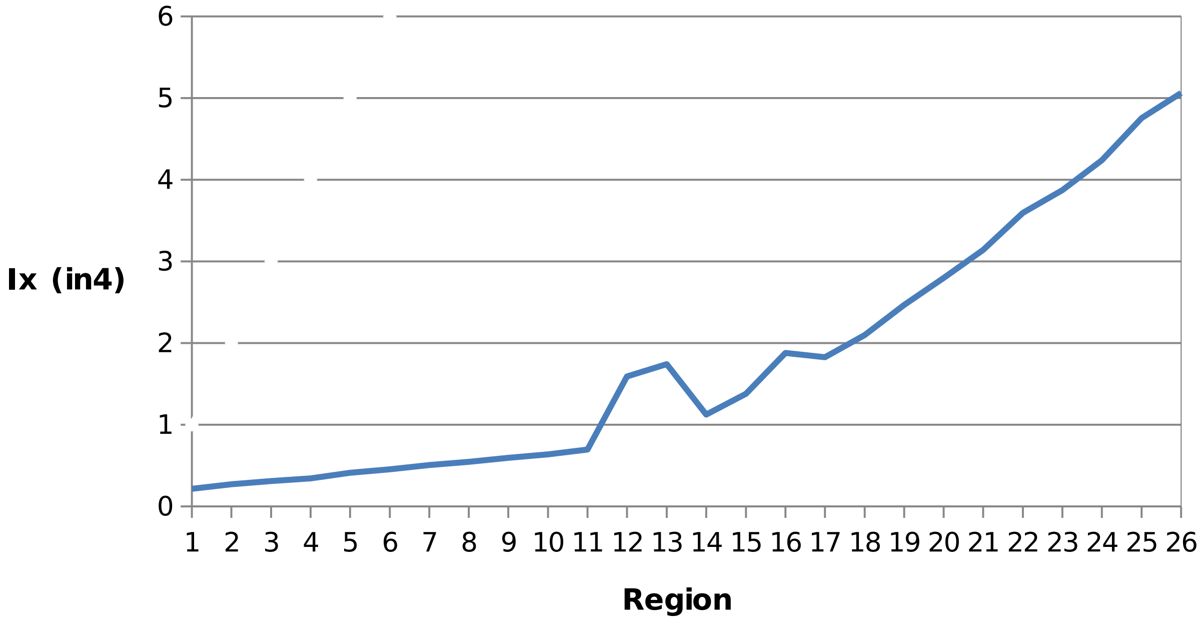

Figure 4-6: Total Moment of Inertia I_X without the Skin

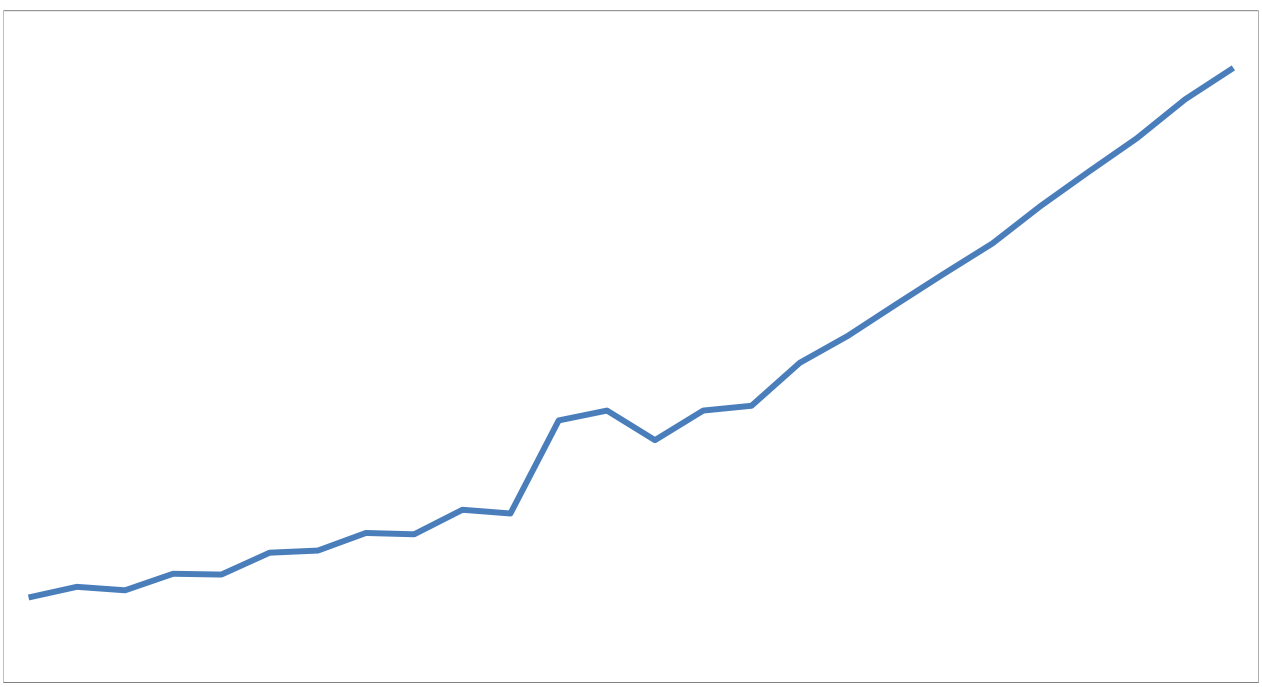

Figure 4-7: Total Moment of Inertia I_Y without the Skin

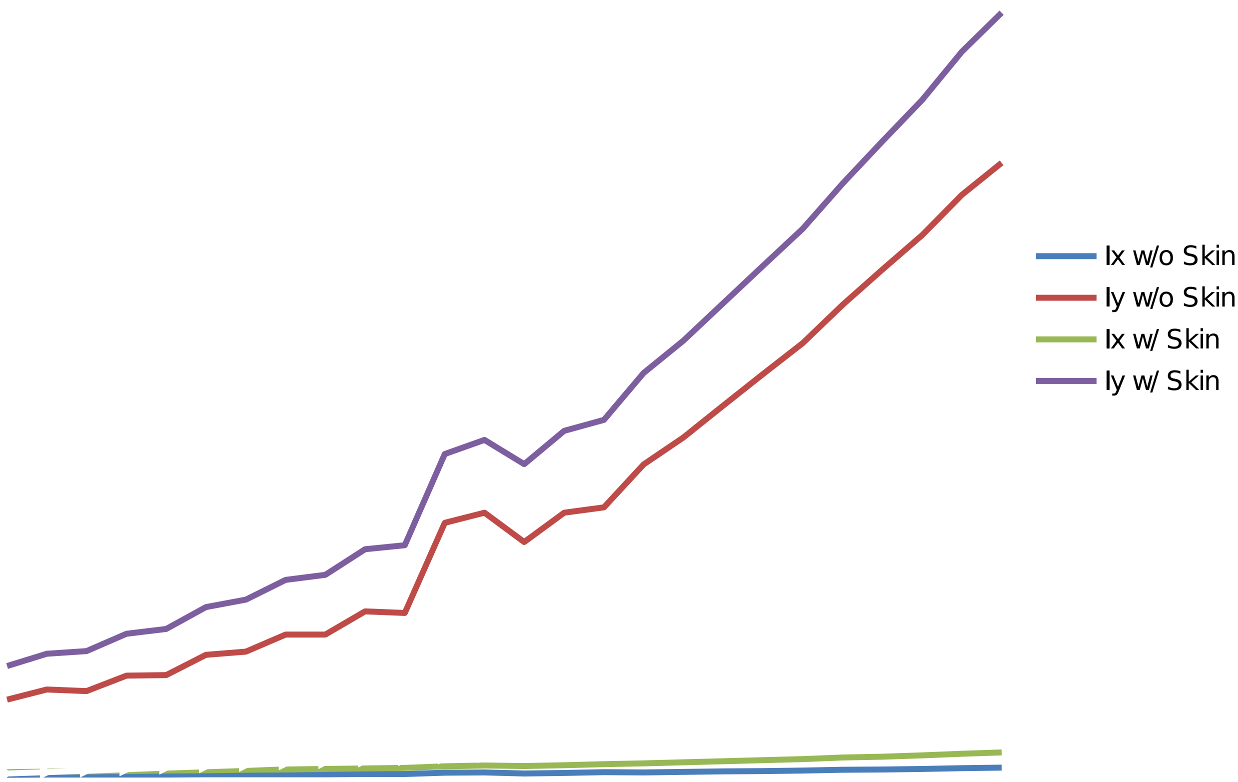

Figure 4 8: Total Moment of Inertial I_x and I_y with and without the Skin

The following shown the moment of inertia, plotted by the distance from the wingtip:

Distance from tip (inches)	I_x	I_y
15.375	2.07998	75.0513
18.375	2.31914	83.59751
21.375	2.544591	85.2867
24.375	2.792224	97.26728
27.375	3.082493	100.5729
30.375	3.359834	115.6674
33.375	3.620504	120.7894
36.375	3.891517	134.3413
39.375	4.251628	137.8814
42.375	4.524098	155.529
45.375	4.920047	158.1977
48.375	6.071853	220.958
51.375	6.559471	230.6673

54.375	6.236375	214.086
57.375	6.845635	237.0648
60.375	7.473282	244.5352
63.375	8.078423	276.8463
66.375	8.772976	299.1138
69.375	9.492067	324.9038
72.375	10.24794	350.7029
75.375	11.07015	376.1652
78.375	12.01784	407.3245
81.375	12.67662	436.3683
84.375	13.55707	464.8806
87.375	14.63991	497.983
90.375	15.46655	524.8826

Table 4-2: Moment of Inertia by distance from the WingTip

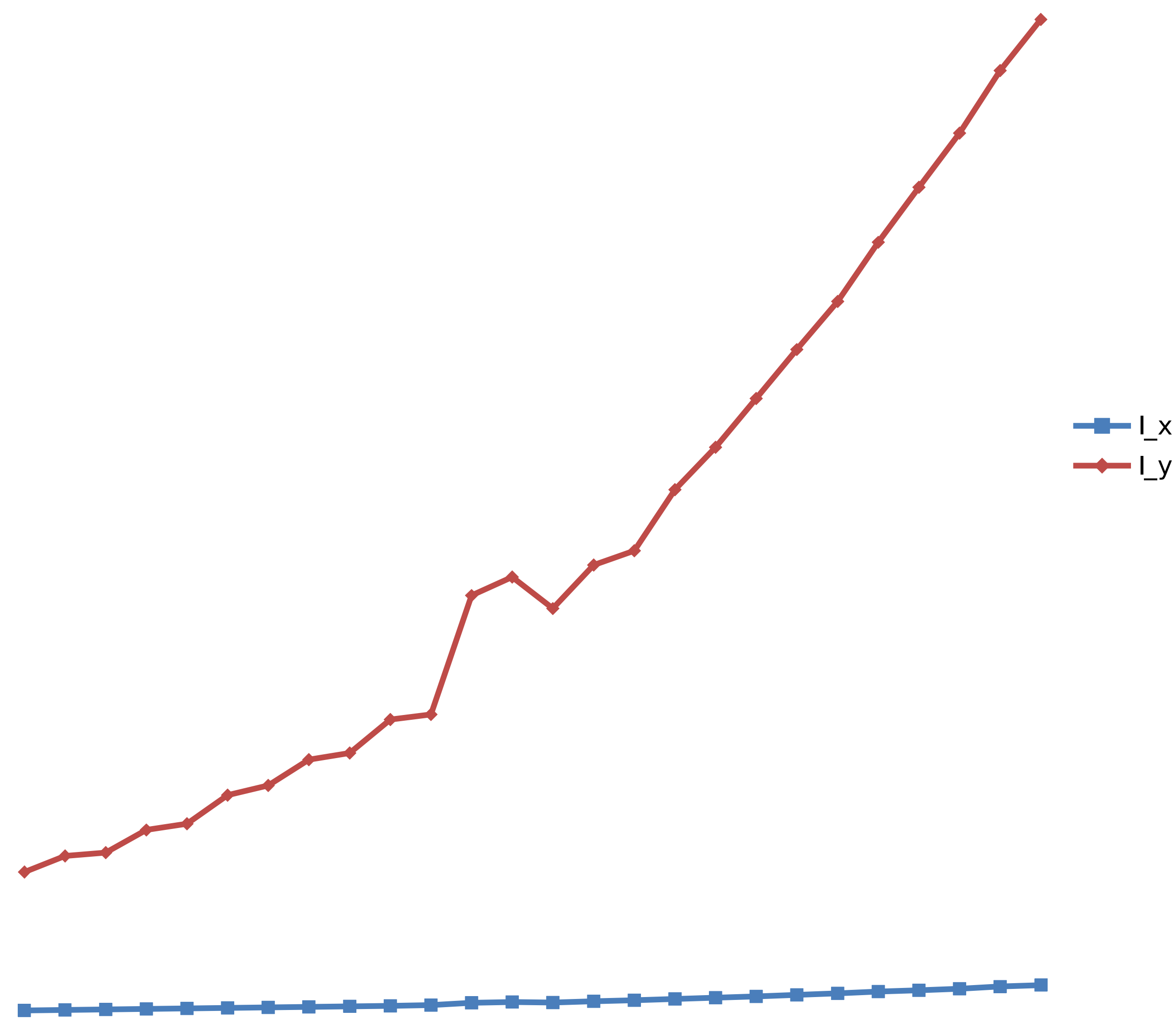

Figure 4-9: Moment of Inertia vs. Distance from WingTip

(From table 4-2)

5.0 EXPERIMENT: FINDING STRESS

Now that we've obtained structure dimensions, centroid, and moment of inertia for each section of the entire wing, we can investigate matching our theoretical values with experimental values. The targets for our experiment are stress and shear center. In order to find these values, we will apply a load on top of the airfoil and obtain readings from the strain gages attached along the wing. The strain gages will be attached on the top, along the skin of the wing, for certain sections. Ultimately, from reading the strain values, we can find the stress and the shear center for any section.

5.1 LOADING METHODS

The following methods will be used to apply loading at certain contact points throughout the tail's top surface:

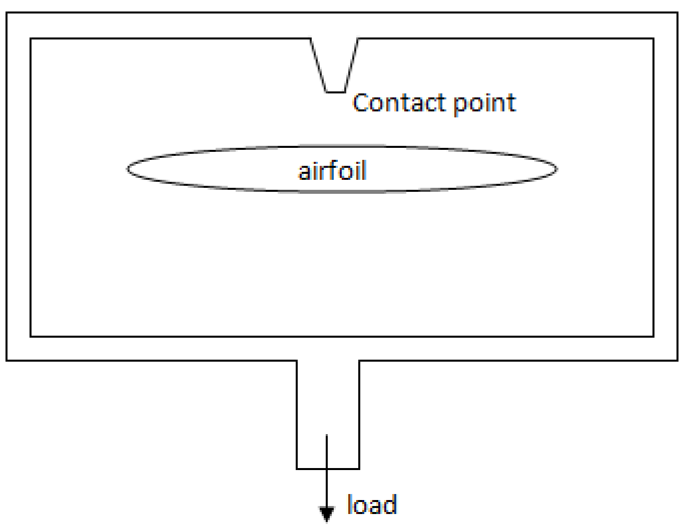

Figure 5-1: Method A

Method A allows freedom to select any point on the tail section to apply load with high precision. It is a stable structure that will not tip toward any direction under vertical axial load. The structure is aluminum with loading weight at bottom. This method will be used to find the shear center.

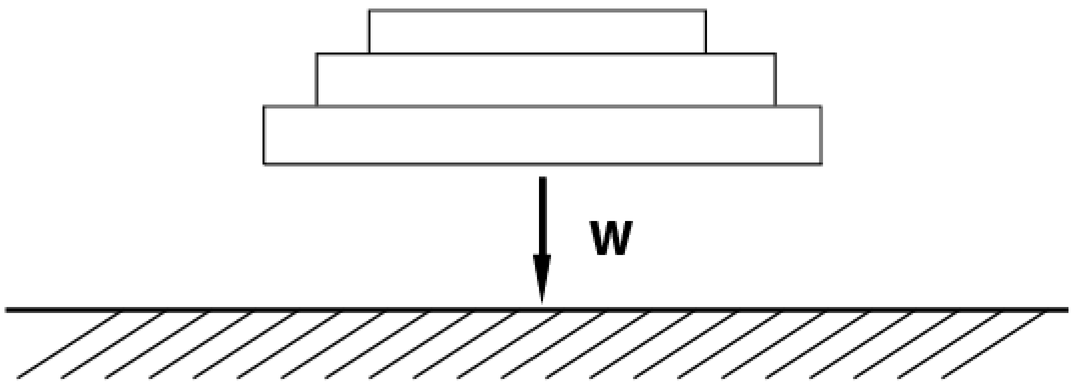

Figure 5-2: Method B

Method B allows same freedom of placement, but it’s practical and easy to apply. This configuration is used to apply direct load on the surface in any generalized area.

5.2 Strain Gages

A strain gage is a device used to measure the strain on the surface of an object. The device measures the electrical conductivity of a string of a metallic foil line placed on the surface with configuration shown below.

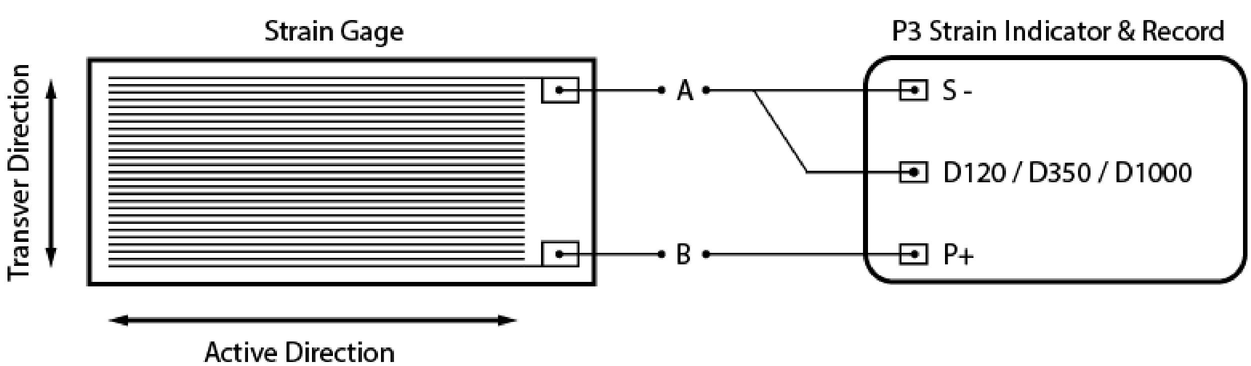

Figure 5-3: Typical Strain Gage Configuration

As the surface expands/compresses upon bending, the resistance through the foil wire changes. As the surface expands, the wire gets thinner and spaces further apart in which the conductivity decreases. When the surface compresses, the wire gets thicker and pushed closer in which conductivity increases. With this device, we can place the strain gage on the surface of the wing and measure the strain when we apply loads on it.

The Rosette Gage has 3 directions to measure strain. The purpose of using the Rosette Gage over the conventional gage is to measure torsion of a structure. If there is no torsion, the reading from two opposing directions (at 45° to the normal direction) will be equal. This is beneficial for us to find the shear center of the structure.

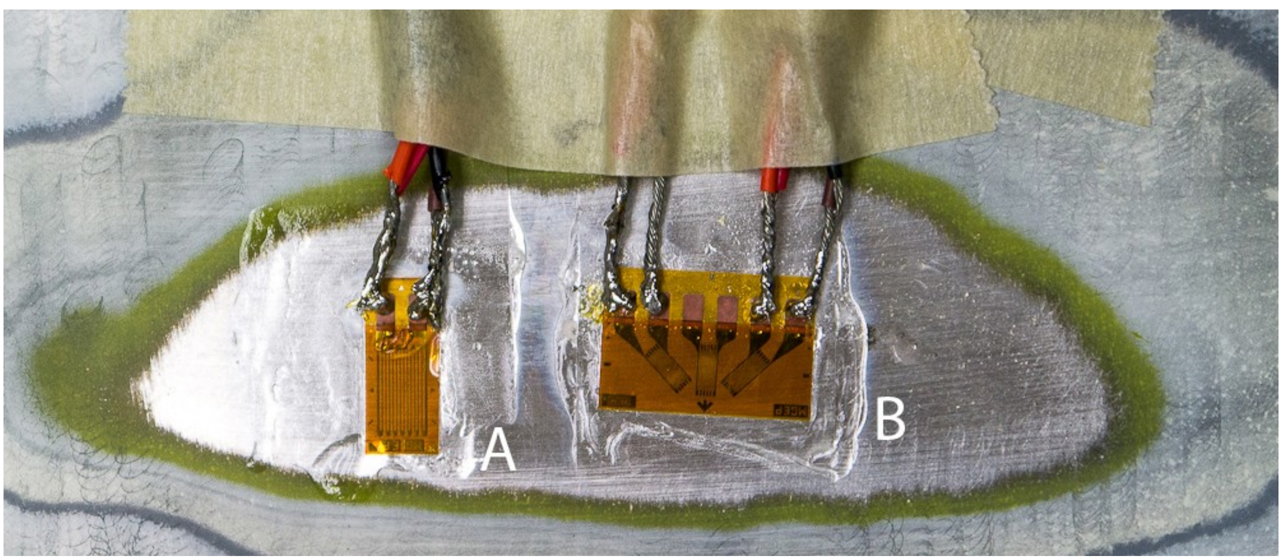

Figure 5-4: Applied Strain Gage; A is a 1 dimensional strain gage and B is a Rosette Gage.

5.2.1 Applying Strain Gages

All the substances, mixed or not mixed, have shelf life of 9 months in tightly closed container at room temperature. Never open a refrigerated bottle until it has reached room temperature.

Substances

1. CSM Degreaser or GC-6 Isopropyl Alcohol
2. Silicon-Carbide Paper
3. M-Prep Conditioner A
4. M-Prep Neutralizer 5A
5. GSP-1 Gauze Sponges
6. CSP-1 Cotton Applicators
7. MJG-2 Mylar® Tape
8. TFE-1 Teflon® Film
9. HSC-X Spring Clamp
10. GT-14 Pressure Pads and Backup Plates

Mixing Instructions:

1. Resin and curing agent bottles must be at room temperature before open
2. Using disposable plastic funnel, empty contents of bottle labeled "Curing Agent" into bottle of resin labeled "Adhesive".
3. After tighten the brush cap, shake this adhesive bottle vigorously for 10 seconds.
4. Mark bottle with date mixed
5. Let the mixed adhesive stand for 1 hour before using.

Surface Preparation: Since our tail section is made of magnesium alloy, we must proceed with cautions since magnesium is prone to catch on fire easily as we sand down and smooth the surface. Start with sand paper with large grit such as 100-grit regular sand paper to get all the paint off the surface until you see the metal with no paint left. After that, use finer sand paper, 220- or 320-grit silicone-carbide paper to smooth the surface. All sanding must be done by hand for safety purposes. Using a hand sander machine may let the tail section catch on fire and is dangerous.

Installing Strain Gages:

1. degrease the gaging are with solvents (CSM Degreaser or GC-6 Isopropyl). Avoid contaminating containers by using “one-way” containers such as aerosol cans.
2. Abrading with 220- or 320-grit silicon-carbide paper to remove any surface scale. After, wet sand with 320- or 400-grit and Prep Conditioner A, followed by a wiping dry with gauze sponge.
3. Apply conditioner A and scrub with cotton-tipped applicator until the clean tip is no longer discolored. Never wipe or scrub back and forth, always go in 1 direction. And never allow any solution to dry on the surface to ensure a good bond after.
4. Apply M-Prep Neutralizer 5A and scrub with a cotton-tipped applicator.
5. Remove the gage from its mylar envelop with tweezers without touching the exposed foil. Place the gage, bonding side down, onto a chemically clean glass plate. Place a short length of MJG-2 mylar tape down over half of the gage tabs and entire terminals.
6. Remove the gage by peeling tape at a shallow angle (30°) and transferring it onto the specimen. Make sure to align the gage accordingly to application purpose. If misplaced, lift the end of the tape at a shallow angle and reapply until the gage is placed correctly.
7. Lift one end of the tape at a shallow angle and raise both gage and terminal with one end of the tape is still in position.
8. Coat the gage backing, terminal, and specimen surface with a thin layer of adhesive. Also coat the foil side of the open-faced gage. Don’t let the adhesive applicator to touch the tape mastic. Let the adhesive to air-dry, by solvent evaporation for 5 – 30 minutes at +24° C and 50% humidity.
9. Return the gage/terminal assembly to its original position over the intended-to-apply area. Use enough pressure with a thumb to allow the assembly to be tacked down. Overlay the gage/terminal area with a piece of thin Teflon sheet

(TFE-1). Apply pressure over the gage for 1 minute to press out all air bubbles.

10. Solder wires into the gage as described in Figure 5-3.
11. Attach the wire into the P3 Strain Indicator as described in Figure 5-3 and take reading.

    Note: Reset values to zero at static position. Apply bending moment to the specimen to see if the P3 Strain Indicator can obtain any values. Return the Specimen to static position, and check if the values return to zero. If the values does not return to zero, that means strain gage has not been installed correctly.

5.3 Strain and Stress

The strain gage will provide reading for $\varepsilon_{\exp}$ the relationship with stress can be expressed as:

$$\sigma_{\exp} = E \cdot \varepsilon_{\exp}$$

Eq. 29

$\sigma_{\exp}$ = experimental value of stress, E = Young's Modulus for Magnesium Alloy,

and $\varepsilon_{\exp}$ = reading from strain gage.

From Young's Modulus table for Magnesium Alloy: 6E6 PSI < $E_{\text{Magnesium Alloy}}$ < 6.5E6 psi

We will be comparing this experimental relationship to our theoretical relationship:

$$\sigma_{th} = \frac{M \cdot y}{I_{\dot{x}}} \qquad \text{Eq. 30}$$

σ_{th} = theoretical value of stress, **M** = moment created by applying weight at the tip of the wing using Method B, **y** = distance between the applied moment and the strain gage, $I_{\dot{x}}$ = the moment of inertial about the neutral axis **X**.

5.4 Results: Experimental vs. Theoretical

station	distant **s** from back plate (member 5, Figure 4-3) (inches)	σ (theoretical)	Strain Gauge Steady Reading (με)	Strain Gauge Instantaneous Reading (με)	σ (experimental) (steady reading)	σ (experimental) (instantaneous reading)
2	N/A		10	N/A	60-65	
4	-6.125	184.36	12	32	72 – 78	192 – 208
7.3	-11	222.44	34	35	204 – 221	210 – 227.5
9	-5.75	205.40	18	22	108 – 117	132 – 143
9	-5.00	205.40	5	22	30 – 32.5	132 – 143
9	-4.50	205.40	10	23	60 – 65	138 – 149.5
11	-7	272.69	25	34	150-162.5	204 – 221
12.5	-7.5	240	40	42	240-260	252 – 273
14.3	-12.5	253.46	37	43	222 – 240.5	258 – 279.5
14.3	-13.75	259.83	40	43	240 – 260	258 – 279.5
18.5	0.2	170.59	25	29	150 – 162.5	174 – 185.5
21	-6.0	229.49	56	56	336 – 364	336 – 364
21	-14.125	235.42	30	40	180 – 195	240 – 260
25.6	0.4	153.90	27	28	162 – 175.5	168 – 182

Table 5-1: Theoretical Stress vs. Experimental Stress

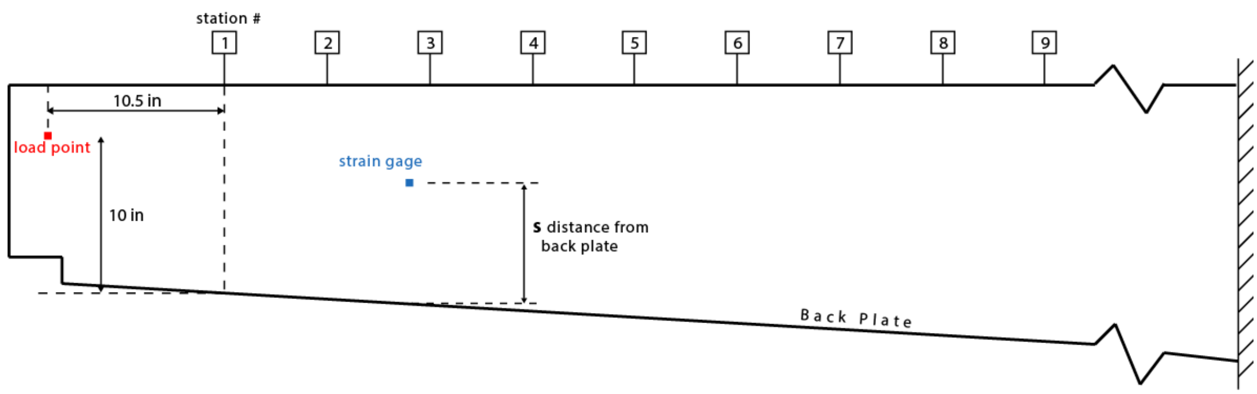

Figure 5-5: Loading Strategy and Strain Gauge Placement

15 lbs is applied at the load point location marked Red in the diagram above. Strain Gauge is indicated in blue showing with **s** distance from the back plate.

6.0 EXPERIMENT: FINDING SHEAR CENTER

6.1 THEORETICAL CALCULATION

Airfoil section under arbitrary bending load:

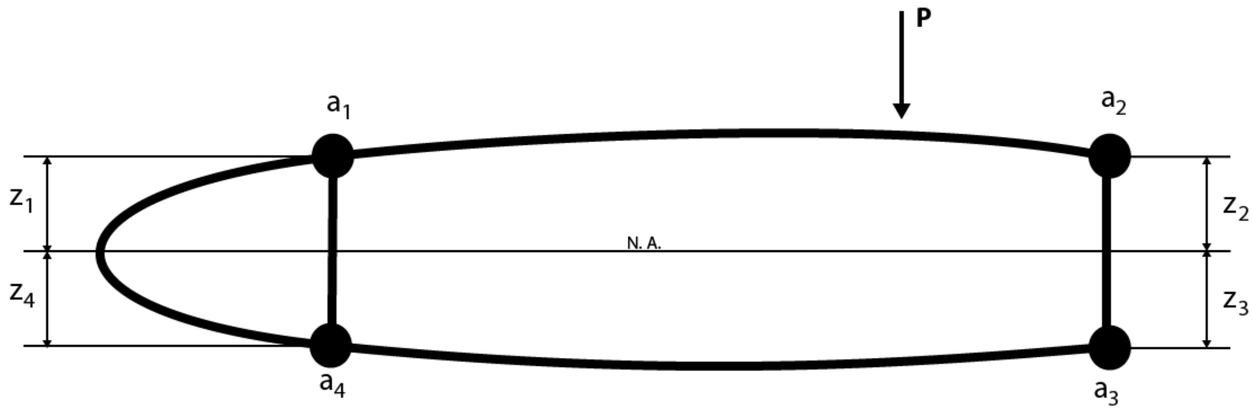

Figure 6-1: General Section

Make two cuts as following:

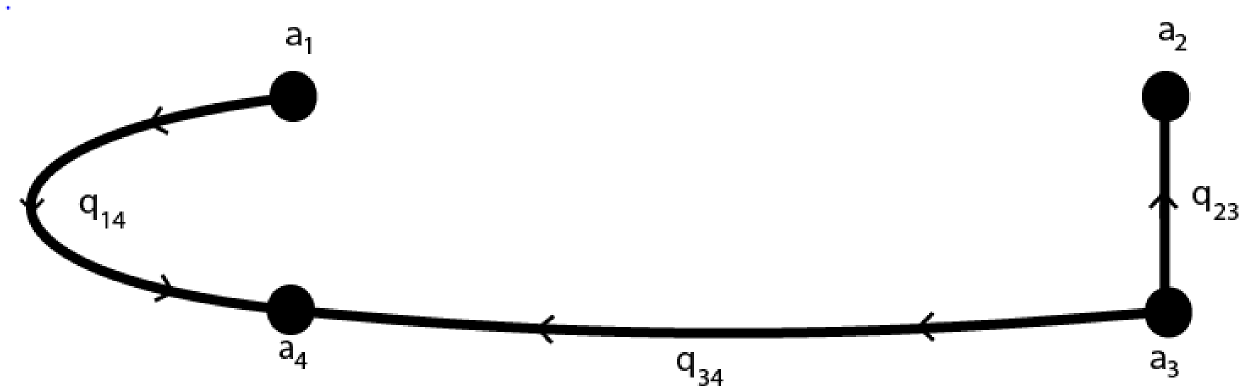

Figure 6-2: Theoretical Cut of two Sections

From our basic static knowledge we can find the shear flow **q** as following:

$$q=\frac{P}{I_{N.A.}}\sum A\cdot z$$

Eq. 31

$$q_{23}=\frac{P}{I}\left(a_2\cdot z_2\right)$$ Eq. 32

$$q_{34}=q_{23}+\frac{P}{I}\left(-a_3\cdot z_3\right)=\frac{P}{I}\left(a_2\cdot z_2-a_3\cdot z_3\right)$$ Eq. 33

$$q_{14}=\frac{P}{I}\left(a_1\cdot z_1\right)$$ Eq. 34

$$q_{34}=q_{14}+\frac{P}{I}\left(-a_4\cdot z_4\right)$$ Eq. 35

After that, we set **Eq. 33** = **Eq. 35** and check if they're compatible.

Check if equilibrium is satisfied: $\sum F_x=0$ $\sum F_z=0$ $\sum M=0$

Check compatibility: $\theta_1=\theta_2=\frac{1}{2AG}\sum\frac{qL}{t}$

Eq. 36

Add **q'₁** and **q'₂** so that solution included **q** from cuts **+ q'** to achieve equilibrium and compatibility:

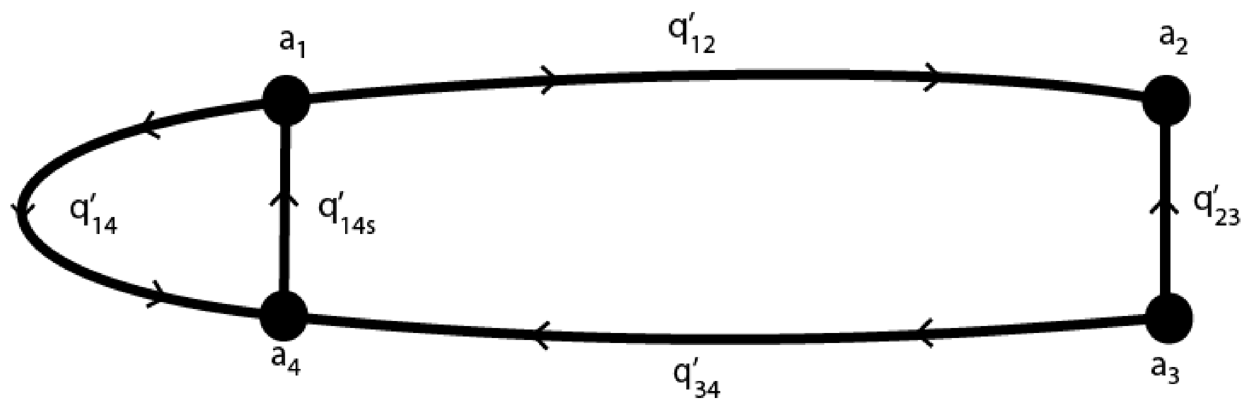

Figure 6-3: Simplified Solution Diagram

To find shear center, assume a shear center position and solve for distance **d** that keep the structure in equilibrium without torsion.

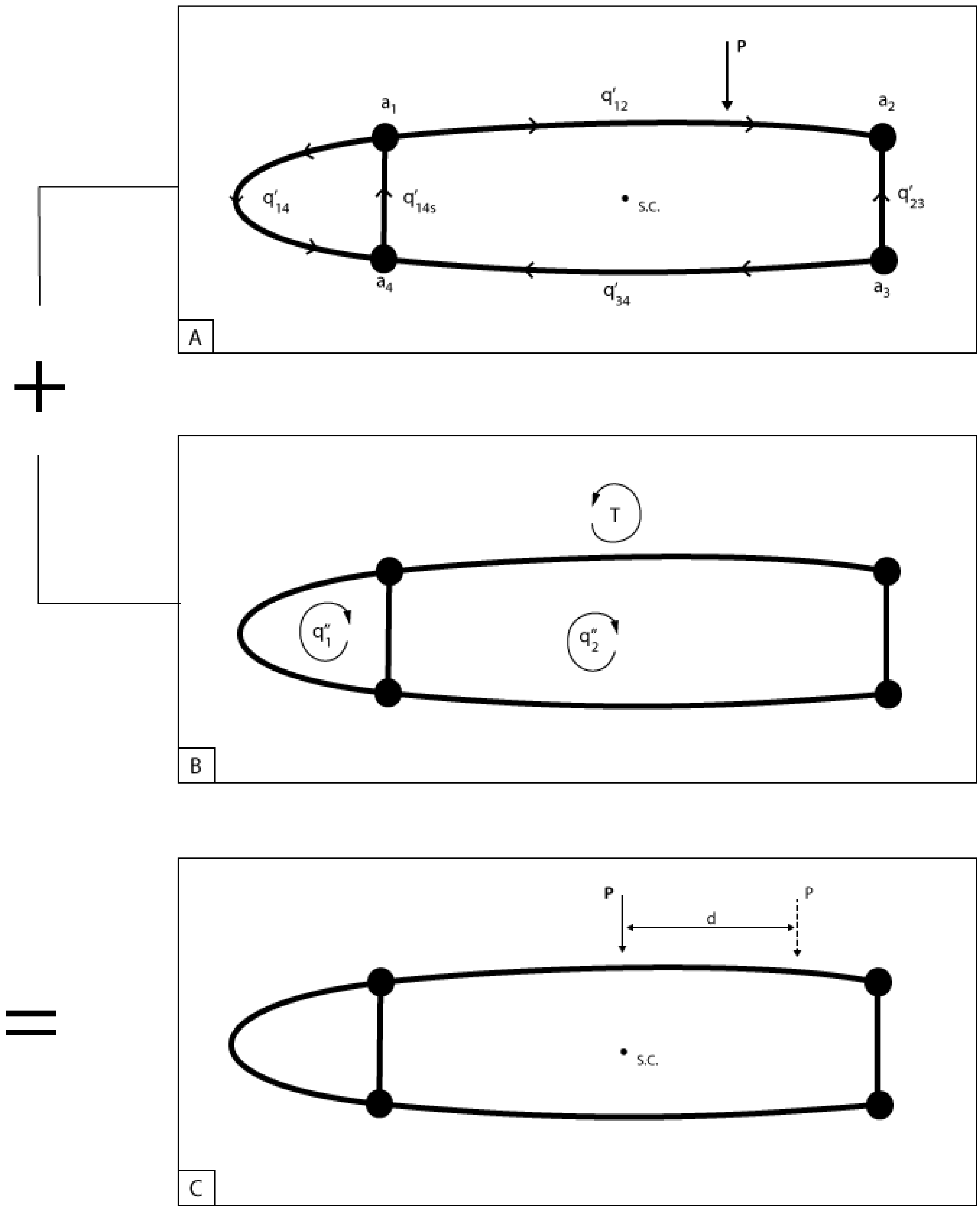

Figure 6-4: Generalizing the Method

At shear center

qL} over {t}}
¿

$$\theta_1=\theta_2=0=\frac{1}{2AG}\sum ¿$$ Eq. 37

qL} over {t}}
¿

$$A_1\theta_1=A_2\theta_2=0=\frac{1}{2G}\sum ¿$$ 1 equation, 2 unknows

Eq. 38

$$\sum M_{any\,stringer}=0$$ 1 equation Eq. 39

6.2 Numerical Calculation (Station 4)

Let's take station 4 and apply the method above. First, find the total area and centroid of each stringer a1, a2, a3 and a4 as Figure 6-3:

a$_1$ = **a**$_4$ **a**$_2$ = **a**$_3$ Similarity: $\acute{x}_{a1}=\acute{x}_{a4}$ $\acute{y}_{a1}=-\acute{y}_{a4}$

$\acute{x}_{a2}=\acute{x}_{a3}$ $\acute{y}_{a2}=-\acute{y}_{a3}$

Dimensioning from Appendix B, Appendix C, Figure 4-3, and Figure 4-4

a$_1$ = **a**$_4$ = $a_6 + a_7 + 0.5a_8 + a_{12+} + 0.5a_{14}$ = 0.2684735

a$_2$ = **a**$_3$ = $a_1 + a_3 + 0.5a_5$ = 0.16944

$$\acute{x}_{a1}=\acute{x}_{a4}=\frac{a_6x_6+a_7x_7+0.5a_8x_8+a_{12}x_{12}+0.5a_{14}x_{14}}{a_6+a_7+0.5a_8+a_{12}+0.5a_{14}}=-17.6058$$

$$\acute{y}_{a1}=-\acute{y}_{a4}=\frac{a_6y_6+a_7y_7+0.5a_8\left(0.5T_3-t_g-t_h-t_i-t_j\right)+a_{12}y_{12}+0.5a_{14}\left(\frac{T_3}{4}\right)}{a_6+a_7+0.5a_8+a_{12}+0.5a_{14}}=0.762886$$

$$\acute{x}_{a2}=\acute{x}_{a3}=\frac{a_1x_1+a_3x_3+0.5a_5x_5}{a_1+a_3+0.5a_5}=9.23666$$

$$\acute{y}_{a2} = -\acute{y}_{a3} = \frac{a_1 y_1 + a_3 y_3 + 0.5 a_5 \frac{T_2}{4}}{a_1 + a_3 + 0.5 a_5} = 1.1683$$

$z_1 = z_4 = 0.762886$

$z_2 = z_3 = 1.1683$

From the output above, we should get:

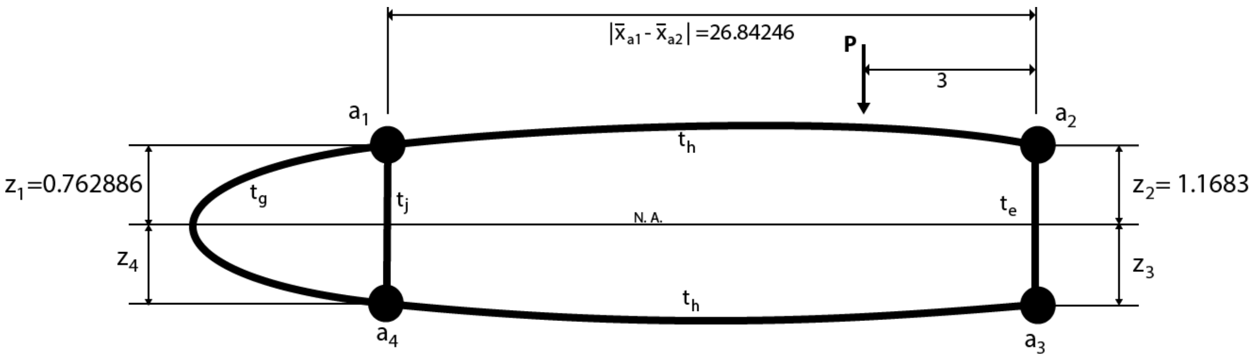

Figure 6-5: Dimension of Station 4 with arbitrary loading P

P = 10 lbs

From Appendix B, the thicknesses are:

t_g	0.04
t_j	0.019573
t_h	0.03
t_e	0.020
I_x	2.792224

Make 2 cuts:

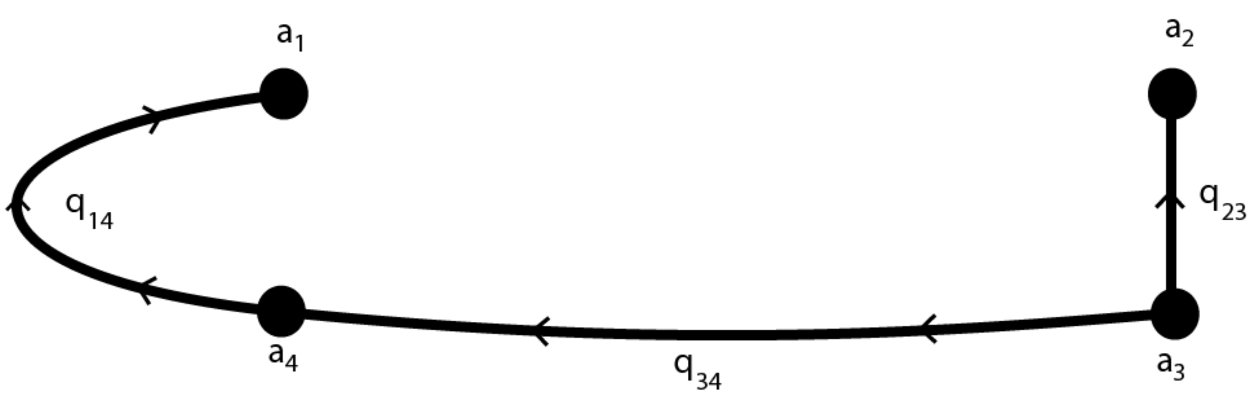

Figure 6-6: Numerical Calculation Cut

Moment of Inertia at Neutral Axis with Approximation from a_1, a_2, a_3, and a_4:

$$I_{N.A.} = \sum a_i z_i^2 = 2\left(0.2684735 \cdot 0.762886^2 + 0.16944 \cdot 1.1683^2\right) = 0.77505$$

$$q = \frac{P}{I_{N.A.}} \sum Az$$

Eq. 40

0.16944
¿
1.1683

$$q_{23} = \frac{10\,lbs}{0.77505} ¿$$

Eq. 41

0.16944
¿
−1.1683

$$q_{34} = q_{23} + \frac{10\,lbs}{0.77505} ¿$$

(symmetry) Eq. 42

0.2684735
¿
0.762886

$$q_{14} = \frac{10\,lbs}{0.77505} ¿$$

Eq. 43

0.086252
¿
−0.943665

$$q_{34} = q_{14} + \frac{10\,lbs}{0.616161} ¿$$

(symmetry) Eq. 44

Put the Top Skin back and find Compensating Shear Flow:

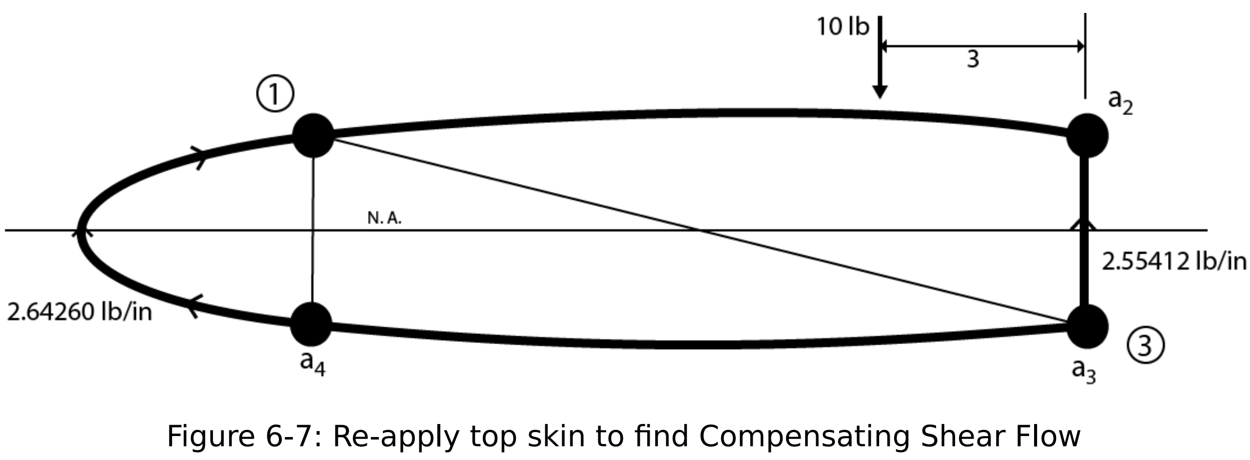

Figure 6-7: Re-apply top skin to find Compensating Shear Flow

$$M = 2qA$$

Eq. 45

$$2\,AG\theta = \sum \frac{qL}{t}$$

Eq. 46

Check Equilibrium:

$$\sum F_z = (2.64260)(0.762886) + (2.64260)(-0.762886) = 0$$ ok Eq. 47

$$F_z = ¿(-10\,lb) + (2.64260)(2\cdot 0.762886) + (2.55412)(2\cdot 1.1683) = -3.8121\cdot 10^{-5}$$
$$\sum ¿$$ Eq. 48

$$\sum M_3 = (10)(3) - (2.64260)\left[\pi\cdot 0.762886^2 + \frac{(2)}{2}(0.762886 + 1.1683)(26.84246)\right] = -111.8182$$

Eq. 49

Check Compatibility:

$$G\theta_1 = \frac{1}{2A_1}\sum \frac{qL}{t} = \frac{1}{\pi(0.762886)^2}(2.6426)\left(\frac{\pi(2)(0.762886)}{2(0.04)}\right) = 86.5988$$ ↻

Eq. 50

$$G\theta_2 = \frac{1}{2A_2}\sum \frac{qL}{t} = \frac{1}{2(51.8378)}(2.55412)\left(\frac{2(1.1683)}{0.02}\right) = 2.8782$$ ↺

Eq. 51

Not Okay

Add q_1' and q_2' so that $G\Theta_1 = G\Theta_2$:

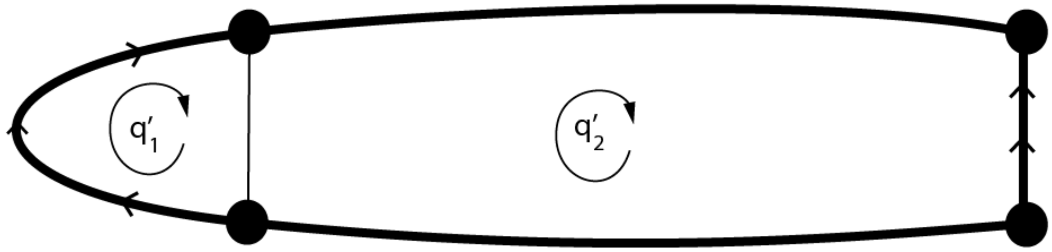

Figure 6-8: Shear Flow of Two Sections

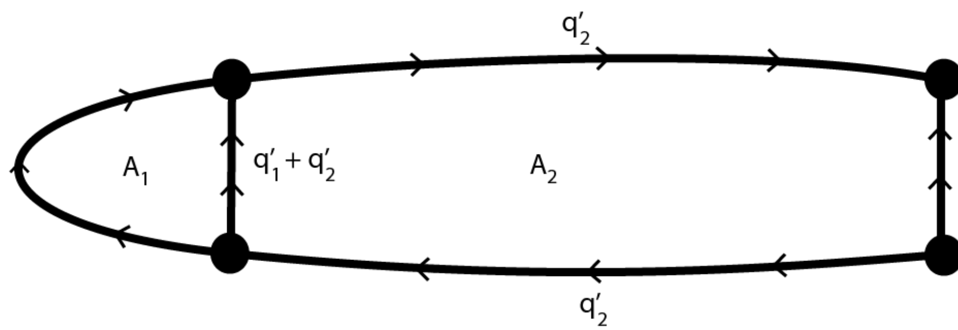

Figure 6-9: Shear Flow Diagram

A_1 = 0.9142 **A_2** = 51.8378

$$G\theta_1=\frac{1}{2A_1}\left[\frac{-(2.6426-q_1')(0.762886\pi)}{0.04}+\frac{(q_1'+q_2')(2)(0.762886)}{0.019573}\right]$$

Eq. 52

$$G\theta_1=\left(\frac{0.762886\pi}{2A_1(0.04)}+\frac{0.762886}{A_1(0.019573)}\right)q_1'+\left(\frac{0.762886}{A_1(0.019573)}\right)q_2'-\frac{0.762886\pi(2.6426)}{2A_1(0.04)}$$

$$G\theta_1=(75.4046)q_1'+(42.6345)q_2'-86.5984$$

Eq. 53

$$G\theta_2=\frac{1}{2A_2}\left[\frac{-(q_1'+q_2')(2)(0.762886)}{0.019573}-\frac{q_2'(26.84246)}{0.03}+\frac{(2.55412-q_2')(2)(1.1683)}{0.02}-\frac{q_2'26.84246}{0.03}\right]$$

Eq. 54

$$G\theta_2=\left(\frac{-0.762886}{A_2(0.019573)}\right)q_1'+\left(\frac{-0.762886}{A_2(0.019573)}-\frac{26.84246}{A_2(0.03)}-\frac{1.1683}{A_2(0.02)}\right)q_2'+\frac{1.1683}{A_2(0.02)}(2.55412)$$

$$G\theta_2=(-0.7519)q_1'+(-19.1393)q_2'+2.8782$$

Eq. 55

Set GΘ1 = GΘ2, to find one equation, 2 unknowns: (set Eq. 53 and Eq. 55 equal)

$$G\theta_1 = G\theta_2 \qquad (75.4046)\,q_1' + (42.6345)\,q_2' - 86.5984 = (-0.7519)\,q_1' + (-19.1393)\,q_2' + 2.8782$$

$$76.1562\,q_1' + 61.7738\,q_2' = 89.4766$$ Eq. 56

Use Moment equation to find one more equation with 2 unknowns:

$$\sum M_3 = -\left(2.6426 - q_1'\right)(2\cdot 53.6662) - \left(q_1' + q_2'\right)(2\cdot 0.762886)(26.84846) - (1.1683)\left(q_2'\right)(26.84246) + (10)(3) = 0$$

Eq. 57

$$0 = [2(53.6662) - 2(0.762886)(26.84246)]\,q_1' + [-2(0.762886)(26.84246) - 1.1683(26.84246)]\,q_2' + [30 - 2.6426(2)($$

$$66.3769\,q_1' - 72.3155\,q_2' = 95.0806$$ Eq. 58

With Eq. 56 and Eq. 58, we have 2 equations and 2 unknowns, we can solve for q_1' and q_2' using matrix properties:

$$\begin{bmatrix} 76.1562 & 61.7738 & 89.4766 \\ 66.3769 & -72.3155 & 95.0806 \end{bmatrix} \xrightarrow{\text{RREF}} \begin{bmatrix} 1 & 0 & 1.0468 \\ 0 & 1 & -0.4679 \end{bmatrix}$$

Results:

$$q_1' = 1.2848$$ (lb/in) Eq. 59

$$q_2' = -0.1355$$ (lb/in)

Eq. 60

Now this section is in equilibrium as following:

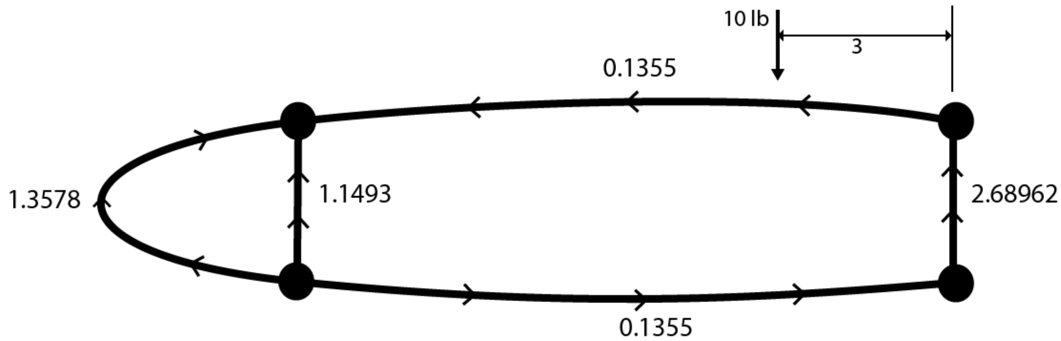

Figure 6-10: Shear Flow Solution Diagram

To find shear center, move load to shear center and solve for distance **d**, which keeps section in equilibrium; no torsion:

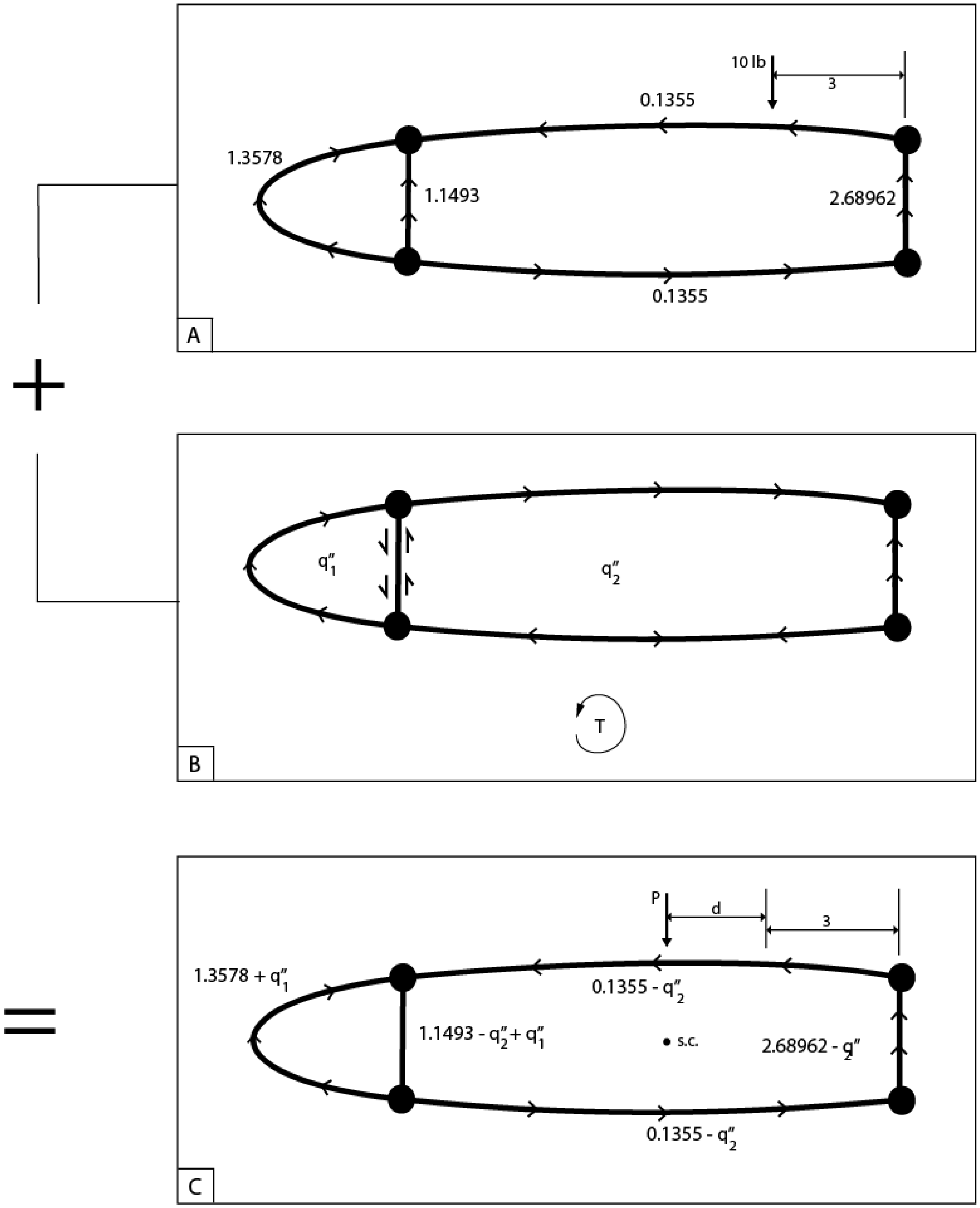

Figure 6-11: Method to locate the Shear Center

Check $\mathbf{q_1'}$ and $\mathbf{q_2'}$ integrity:

$G\theta_1 = (75.4046)\,q_1' + (42.6345)\,q_2' - 86.5984 = 4.5045$ Very close to $G\theta_2$

$G\theta_2 = (-0.7519)\,q_1' + (-19.1393)\,q_2' + 2.8782 = 4.5055$ Very close to $G\theta_1$

-72.3155
¿q
¿
$\sum M_3 = (66.3769)\,q_1' +$ ¿ Almost zero for equilibrium

Find q_1'' and q_2'' which exactly cancel $G\theta_1$ and $G\theta_2$:

}) left [{0.762886π} over {0.04} + {2·0.762886} over {0.019573} right]
$q_1^{¿}$
$4.5045 = G\theta_1 = \frac{1}{2A_1}$ ¿

} =0.0597
→ $q_1^{¿}$ (lb/in)

}) left [{2(0.762886)} over {0.019573} + {2(26.84246)} over {0.03} + {2(1.1683)} over {0.020} right]
$q_2^{¿}$
$4.5055 = G\theta_2 = \frac{1}{2A_2}$ ¿

} =0.2354
→ $q_2^{¿}$ (lb/in)

From Figure 6-11, we have this:

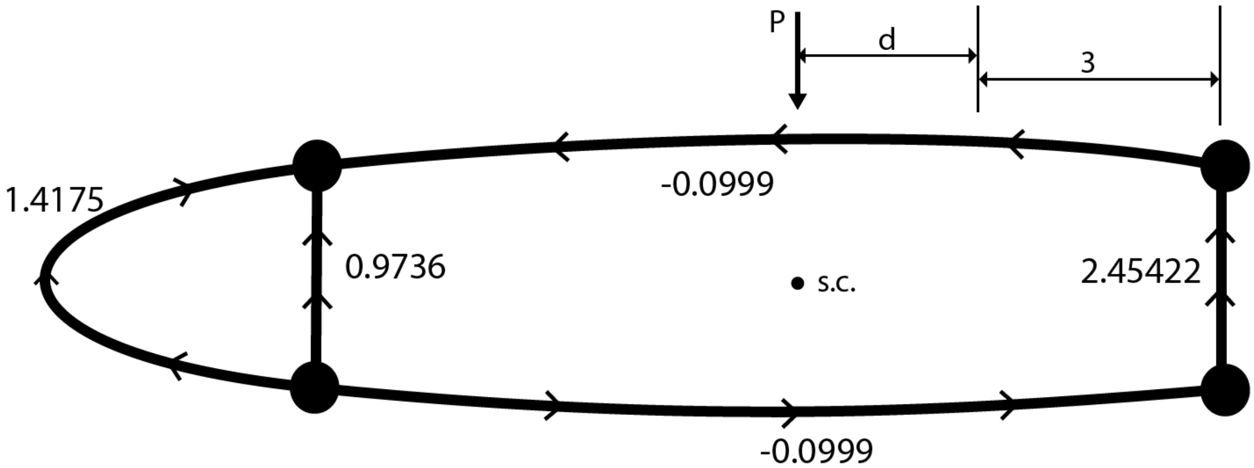

Figure 6-12: True Shear Flow

$$\sum M_3 = (-1.4175)\left(0.9142 + \frac{51.8378}{2}\right) - (0.9736)(2)(0.762886)(26.84246) + (-0.0999)(26.84246)(2)(1.1683) + 10$$

$$d = 5.4176$$

Shear center location $¿ d + 3 = 5.4176 + 3 = 8.4176$ inch

The shear center is about $\boxed{8.4176 \text{ in}}$ from the right side

6.3 EXPERIMENTAL RESULTS

We used our designed loading device to apply the load onto the wing to find the shear center. See Appendix E for the CAD drawing of the loading device. Our device will apply the load at the tip to precisely locate the shear center location. When the loading device is on the wing, we can simply move it from one location to another until the Rosette Gage shows equal reading from both directions; which indicates that there is no torsion present, thus the shear center is found.

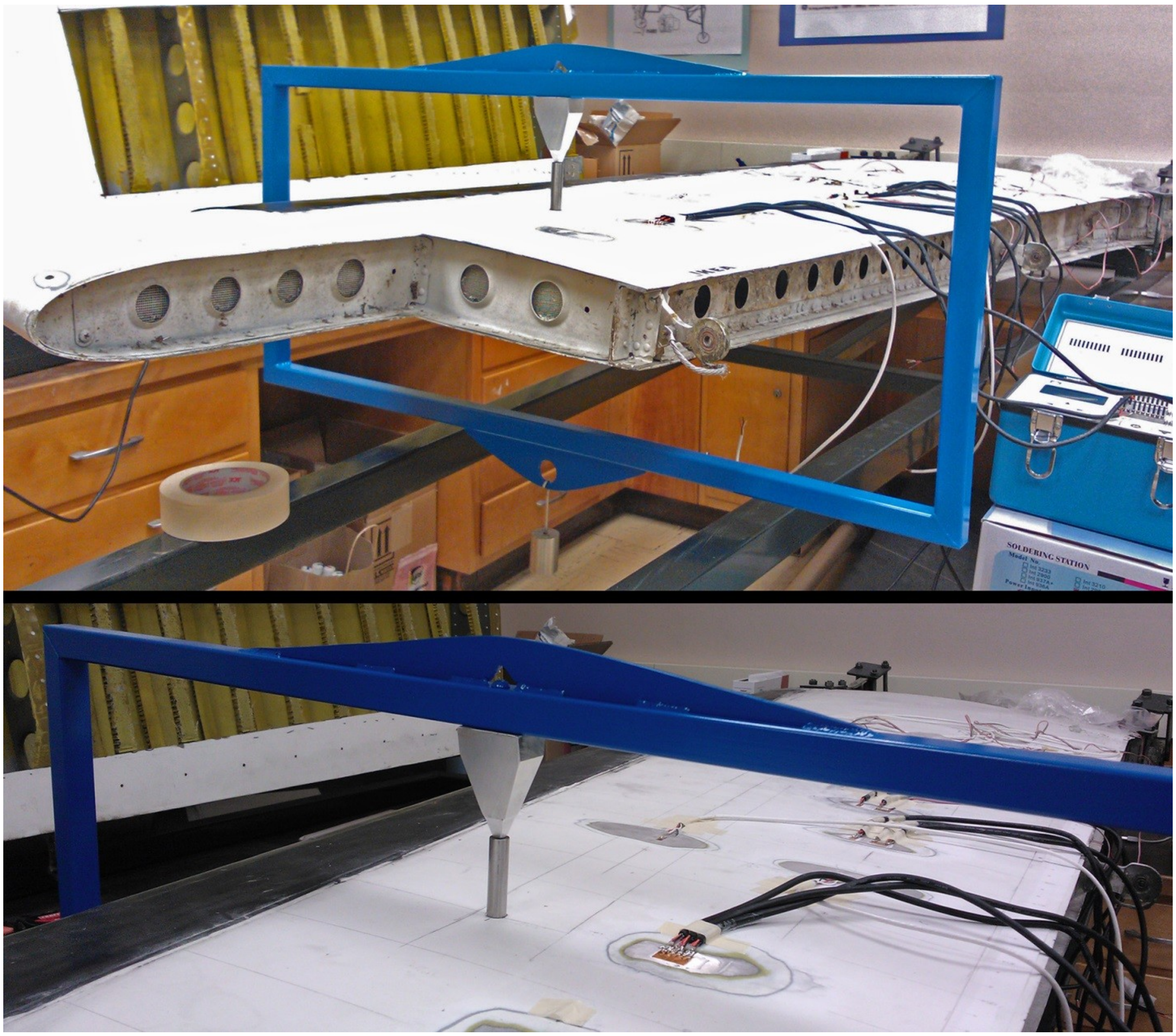

Figure 6-13: Loading Device Applied on the Wing

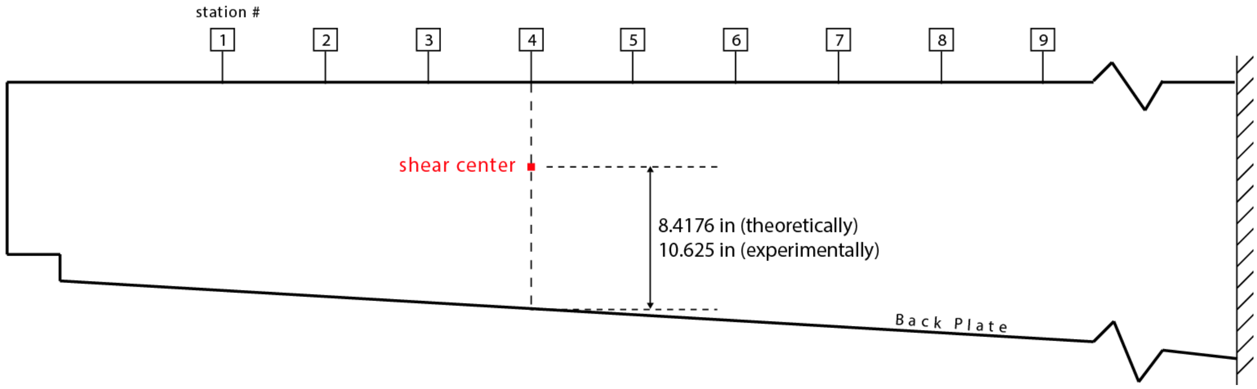

Figure 6-14: Shear Center Location

We found the shear center is located $\boxed{\text{-10.625 in}}$ from the Back Plate (member 5 in the cross section diagram, Figure 4-3). This is marginally acceptable from our Theoretical Calculation value of $\boxed{\text{8.4176 in}}$.

7.0 CONCLUSION

7.1 DATA OBTAINED

I have successfully measured and obtained all dimension values of the tail section. The excel sheet (Appendix B, C & D), demonstrated that obtaining the moment of inertia through precise measurement of each cross section is feasible. Moreover, all values obtained are reasonable. Moment of inertia increases toward the root as it should.

As expected, as we go toward the root of the tail section, the area for each cross section increases, and the distance between the elements increases as well. For this reason, the moment of inertia increases rapidly toward the root of the tail section. At region 12 and 13, we saw a significant increment of moment of inertia. This is due to the extra thickness added by the hinges to support the flaps.

7.2APPLIED STRESS AND STRAIN GAGES

When we applied the strain gages, there are a few problems leading to our inaccurate reading:

- Our adhesive method does not hold the strain gage for prolong period of time
- The strain gage stayed attached for a short amount of atime

As stated above, since the strain gages do not hold for a prolong period of time. To verify this phenomenon, we take 2 readings from the strain gages: (1) Instantaneously and (2) Steady State. The instantaneous reading is taken within 2 second after the load has been applied. The Steady State reading is taken 1 min after the load has been applied. As we can see in Table 5-1, the instantaneous gave a much more accurate reading of the stress and is marginally acceptable. However, the Steady State reading is almost completely off scale and the values decreased greatly. This proves that either: (1) one of our steps applying the strain gage has been misconduct, or (2) our adhesive (Kazy Glue) were not good, or (3) the strain gages have been stretched.

7.3 SHEAR CENTER

The calculation from Section 6.2 is marginally acceptable with the experimental results from Section 6.3 for the following reasons:

- As the loading device being placed, it depress an area of the surface; hence, effecting the reading on the strain gages applied on the same surface
- The wing is not entirely Magnesium; the Stringers might be made of Aluminum (unconfirmed). The calculation is based on the assumption that the entire wing material properties of Magnesium for E = 6E6

- The leading stringers' centroid is the combination of the leading edge's skin's centroid, approximated in parabolic form and integrated into the leading stringers.
- The trailing stringers are the combination of multiple supporting plates and wing skins at the region and the rear stringers.

For the reasons stated above, the error of 20% is reasonable to accept and enough for us to prove that, the classical approach of finding the shear center does work if our approximation is accurate enough and the simplification of the problem should be valid.

Given the amount of time, it is impossible to accurately measure the leading edge centroid according to its true geometry, so using parabolic function to approximate its location and semi-circle to approximate its area in shear flow calculation made it possible to finish in a reasonable amount of time.

8.0 References

(2012, February 25). Retrieved March 5, 2012, from Airfoil Investigation Database: http://worldofkrauss.com/

Atmeh, M. G., Hassan, Z., & Darwish, F. (2010). Design and Stress Analysis of a General Aviation Aircraft Wing. *COMSOL* (p. 7). Boston: Jordan University of Science and Technology.

Crawford, D. N. (2002). *Load Pad Development for Research Aircraft Wing Strain Gage Loads Calibration Test.* Edwards: NASA.

Engineering, R. (2009, April 29). Beechcraft Super King Air Models 200/200C/B200/B200C. *Manual* . 09EA-52-116, FAA: Beechcraft.

Gaunt, J. D., Flores, J. C., & Perry, V. A. (2010). *Analysis of a Small Scale Composite Wing.* San Luis Obispo: California Polytechnic State University.

Hibbeller, R. C. (2007). *Engineering Mechanics Dynamics.* Upper Saddle River: Pearson Prentice Hall.

Juraeka, D., & Jekacek, D. (2000). *Strength Test of the UFM-10 Samba Composite Wing Structure.* IAE Brno TU.

Ko, L. W., & Jenkins, M. J. (1987). Thermal Stress Analysis of Space Shuttle Orbiter Wing Skin Panel and Thermal Protection System. *NASA Technical Memorandum 88276* , 23.

Kriz, R. D. (1973). *Static Stress Analysis of a Sailplane Wing Constructed of Composite Materials.* San Luis Obispo: California Polytechnic State University.

Lednicer, D. (2010, September 15). *The Incomplete Guide to Airfoil Usage*. Retrieved March 6, 2012, from UIUC Airfoil Data Site: http://www.ae.illinois.edu/m-selig/ads/aircraft.html

Lokos, W. A., Olney, C. D., Chen, T., & Crawford, N. D. (2002). Strain Gage Loads Calibration Testing of the Active Aeroelastic Wing F/A-18 Aircraft. *NASA STI Program* , 17.

Paur, J. (2010, March 29). Boeing 787 Passes Incredible Wing Flex Test. *Wired* , p. 1.

Saric, W. S., Carpenter, A., Hunt, L., McKnight, C., & Schouten, S. (2006). *SWIFT Safety Analysis for Sweept-Wing Experiments.* College Station: Texas A&M University System.

Wang, J., & Joseph, D. D. (2005). *The lift, drag and torque on an airfoil in foam modeled by the potential flow of a second-order fluid.* Edwards: Fluid Mech.

Appendix A: Equations for Dimensioning

Formulas	Elements (x)
$a_1 = w_a \bullet t_a$	a_1
$x_1 = t_a/2$	x_1
$y1 = (T_2/2) - (w_a/2)$	y_1
$x_{c1} = x_1 - X$	x_{c1}
$y_{c1} = y_1 - Y$	y_{c1}
$a_2 = w_b \bullet t_b$	a_2
$x_2 = t_b/2$	x_2
$y_2 = -(T_2/2) + (w_b/2)$	y_2
$x_{c2} = x_2 - X$	x_{c2}
$y_{c2} = y_2 - Y$	y_{c2}
$a_3 = w_c \bullet t_c$	a_3
$x_3 = t_a + (w_c/2)$	x_3
$y_3 = (T_1/2) - (t_c/2)$	y_3
$x_{c3} = x_3 - X$	x_{c3}
$y_{c3} = y_3 - Y$	y_{c3}
$a_4 = w_d \bullet t_d$	a_4
$x_4 = t_b + (w_d/2)$	x_4
$y_4 = -(T_1/2) + (t_d/2)$	y_4
$x_{c4} = x_4 - X$	x_{c4}
$y_{c4} = y_4 - Y$	y_{c4}

$a_5 = T_2 \cdot t_e$	a_5
$x_5 = -t_e/2$	x_5
$y_5 = 0$	y_5
$x_{c5} = x_5 - X$	x_{c5}
$y_{c5} = y_5 - Y$	y_{c5}
$f_L = (21/44)x + (1663/88)$	f_L
$f_s = (8.625/21.1667)x + 15.3677$	f_S
measured	t_g
measured	t_h
$t_i(x)=(0.005/24.559)x + 0.034122$	t_i
$t_j=(0.035/25.6)x + 0.014104$	t_j
$w_e=(0.358/23.1667)x + 1.37836$	w_e
$w_f=(0.38/21.1667)x + 1.31058$	w_f
$w_g=(0.055/20.1667)x + 0.818239$	w_g
$a_6 = w_f \cdot t_i$	$a_6 = a_{11}$
$x_6 = -f_s + (w_f/2)$	$x_6 = x_{11}$
$y_6 = (T_3/2) - t_g - t_h - (t_i/2)$	$y_6 = -y_{11}$
$x_{c6} = x_6 - X$	$x_{c6} = x_{c11}$
$y_{c6} = y_6 - Y$	$y_{c6} = y_{c11}$
$a_7 = w_g \cdot t_j$	$a_7 = a_{10}$
$x_7 = -f_s + (w_g/2)$	$x_7 = x_{10}$
$y_7 = (T3/2) - t_g - t_h - t_i - (t_j/2)$	$y_7 = -y_{10}$
$x_{c7} = x_7 - Y$	$x_{c7} = x_{c10}$

$y_{c7} = y_7 - Y$	$y_{c7} = -y_{c10}$
$a_8 = t_j \bullet (T_3 - t_g - t_h - t_i - t_j)$ $x_8 = x_9 = -f_s + (t_j/2)$ $y_8 = 0$ $x_{c8} = x_8 - Y$ $y_{c8} = y_8 - Y$	$(2/5)a_8 = a_9$ $x_8 = x_9$ $y_8 = y_9$ $x_{c8} = x_{c9}$ $y_{c8} = y_{c9}$
$L = f_L - f_S + w_e$ A_{fh1} [a to b] = A_{fh1} [c to d] = $a_{12} = a_{13}$ A_{fh1} [b to c] = Eq. 12 A_{fh2} [b to c] = Eq. 13 $f_{h1}(y) = (-4L/T_3^2)y^2 + L$ $f_{h2}(y) = [-4(L - t_g)/(T_3-2t_g)^2]y^2 + (L - t_g)$	L A_{fh1} A_{fh1} A_{fh2} f_{h1} f_{h2}
$a_{12} = a_{13} = A_{fh1} = A_{fh2}$ x_{12} = Eq. 20 y_{12} = Eq. 23 $x_{c12} = x_{12} – X$ $y_{c12} = y_{12} – Y$	$a_{12} = a_{13}$ $x_{12} = x_{13}$ $y_{12} = -y_{13}$ $x_{c12} = x_{c13}$ $y_{c12} = -y_{c13}$
$a_{14} = A_{fh1} - A_{fh2}$ x_{14} = Eq. 27 $y_{14} = 0$ $x_{c14} = x_{14} – X$ $y_{c14} = y_{14} – Y$	a_{14} x_{14} y_{14} x_{c14} y_{c14}

Table A-1: Dimensioning Equations

Appendix B: Measurements

i	t_a	t_b	t_c	t_d	t_e	t_f	t_g	t_h	t_i	t_j
1	0.084	0.073	0.127	0.143	0.020		0.04	0.03	0.034326	0.015471
2	0.084	0.075	0.142	0.152	const		const	const	0.034529	0.016838
3	0.085	0.070	0.142	0.161	▯		▯	▯	0.034733	0.018206
4	0.080	0.077	0.163	0.173		1.476			0.034936	0.019573
5	0.075	0.076	0.188	0.192		1.552			0.03514	0.02094
6	0.088	0.090	0.194	0.205		1.642			0.035344	0.022307
7	0.105	0.100	0.212	0.213		1.712			0.035547	0.023674
8	0.105	0.093	0.221	0.215		1.753			0.035751	0.025042
9	0.110	0.103	0.216	0.236		1.84			0.035954	0.026409
10	0.125	0.110	0.232	0.230		1.926			0.036158	0.027776
11	0.114	0.119	0.253	0.246		2.025			0.036362	0.029143
12	0.118	0.120	0.271	0.268		1.66			0.036565	0.03051
13	0.119	0.123	0.282	0.286		1.384			0.036769	0.031877
14	0.130	0.114	0.278	0.271		2.022			0.036972	0.033245
15	0.140	0.122	0.297	0.290		1.99			0.037176	0.034612
16	0.13	0.13	0.30	0.30		2.02			0.037379	0.035979

	4	5	7	6		2				
17	0.133	0.130	0.306	0.307		2.045			0.037583	0.037346
18	0.130	0.132	0.310	0.320		2.083			0.037787	0.038713
19	0.135	0.130	0.331	0.325		2.09			0.03799	0.040081
20	0.135	0.133	0.338	0.338		2.118			0.038194	0.041448
21	0.133	0.133	0.344	0.353		2.102			0.038397	0.042815
22	0.136	0.135	0.354	0.372		2.1			0.038601	0.044182
23	0.136	0.137	0.373	0.371		2.032			0.038805	0.045549
24	0.141	0.135	0.357	0.373		1.935			0.039008	0.046917
25	0.140	0.135	0.369	0.384		1.945			0.039212	0.048284
26	0.137	0.134	0.365	0.372		1.91			0.039415	0.049651

Table B-1: Measurement A

i	w_a	w_b	w_c	w_d	T_1	T_2	T_3
1	0.915	0.935	0.540	0.576	2.61	2.651	2.148376
2	0.704	0.714	0.542	0.598	2.69	2.73	2.213771
3	0.714	0.718	0.552	0.580	2.79	2.82	2.279167
4	0.715	0.721	0.510	0.573	2.881	2.911	2.344562
5	0.735	0.732	0.503	0.570	2.995	3.035	2.409958
6	0.749	0.737	0.491	0.565	3.096	3.124	2.475354
7	0.767	0.745	0.500	0.553	3.172	3.222	2.540749
8	0.767	0.743	0.491	0.543	3.243	3.278	2.606145
9	0.749	0.751	0.477	0.550	3.312	3.355	2.67154
10	0.761	0.740	0.477	0.541	3.399	3.43	2.736936
11	0.767	0.752	0.445	0.532	3.525	3.555	2.802331
12	1.108	1.148	1.065	1.057	3.624	3.693	2.867727
13	1.203	1.175	1.045	1.045	3.718	3.791	2.933123
14	0.898	0.904	0.603	0.640	3.777	3.830	2.998518
15	0.952	0.958	0.660	0.712	3.872	3.926	3.063914

16	0.992	0.114	0.710	0.764	3.977	4.032	3.129309
17	1.017	1.046	0.779	0.817	4.073	4.122	3.194705
18	1.031	1.097	0.853	0.872	4.158	4.212	3.260101
19	1.059	1.148	0.930	0.937	4.259	4.323	3.325496
20	1.110	1.201	1.000	0.983	4.346	4.415	3.390892
21	1.119	1.230	1.057	1.040	4.410	4.490	3.456287
22	1.159	1.295	1.126	1.110	4.482	4.573	3.521683
23	1.212	1.321	1.189	1.160	4.509	4.611	3.587079
24	1.317	1.360	1.262	1.238	4.575	4.649	3.652474
25	1.369	1.422	1.306	1.313	4.662	4.766	3.71787
26	1.426	1.470	1.358	1.378	4.742	4.847	3.783265

Table B-2: Measurement B

Appendix C: Area and Centroid Coordinate

i	a_1	x_1	y_1	x_{c1}	y_{c1}	a_2	x_2	y_2	x_{c2}	y_{c2}
1	0.07686	0.042	0.868	10.11731	0.878426	0.068255	0.0365	-0.858	10.11181	-0.84757
2	0.059136	0.042	1.013	10.00129	1.02638	0.05355	0.0375	-1.008	9.996789	-0.99462
3	0.06069	0.0425	1.053	11.03295	1.062718	0.05026	0.035	-1.051	11.02545	-1.04128
4	0.0572	0.04	1.098	10.51471	1.119464	0.055517	0.0385	-1.095	10.51321	-1.07354
5	0.055125	0.0375	1.15	11.34993	1.174454	0.055632	0.038	-1.1515	11.35043	-1.12705
6	0.065912	0.044	1.1875	10.64129	1.218288	0.06633	0.045	-1.1935	10.64229	-1.16271
7	0.080535	0.0525	1.2275	11.30917	1.238683	0.0745	0.05	-1.2385	11.30667	-1.22732
8	0.080535	0.0525	1.2555	10.99627	1.254793	0.069099	0.0465	-1.2675	10.99027	-1.26821
9	0.08239	0.055	1.303	11.89167	1.336164	0.077353	0.0515	-1.302	11.88817	-1.26884
10	0.095125	0.0625	1.3345	11.30957	1.338507	0.0814	0.055	-1.345	11.30207	-1.34099

11	0.087438	0.057	1.394	12.31462	1.425707	0.089488	0.0595	-1.4015	12.31712	-1.36979
12	0.130744	0.059	1.2925	8.559051	1.291099	0.13776	0.06	-1.2725	8.560051	-1.2739
13	0.143157	0.0595	1.294	9.040813	1.300642	0.144525	0.0615	-1.308	9.042813	-1.30136
14	0.11674	0.065	1.466	11.23392	1.458806	0.103056	0.057	-1.463	11.22592	-1.47019
15	0.13328	0.07	1.487	10.80961	1.483317	0.116876	0.061	-1.484	10.80061	-1.48768
16	0.132928	0.067	1.52	11.52014	1.418888	0.01539	0.0675	-1.959	11.52064	-2.06011
17	0.135261	0.0665	1.5525	10.64147	1.566614	0.13598	0.065	-1.538	10.63997	-1.52389
18	0.13403	0.065	1.5905	10.52752	1.613865	0.144804	0.066	-1.5575	10.52852	-1.53413
19	0.142965	0.0675	1.632	10.30714	1.630885	0.14924	0.065	-1.5875	10.30464	-1.58861
20	0.14985	0.0675	1.6525	10.16046	1.651189	0.159733	0.0665	-1.607	10.15946	-1.60831
21	0.148827	0.0665	1.6855	10.098	1.696408	0.16359	0.0665	-1.63	10.098	-1.61909
22	0.157624	0.068	1.707	9.85737	1.727895	0.174825	0.0675	-1.639	9.85687	-1.6181
23	0.164832	0.068	1.6995	9.772206	1.695273	0.180977	0.0685	-1.645	9.772706	-1.64923

24	0.185697	0.0705	1.666	9.765912	1.67159	0.1836	0.0675	-1.6445	9.762912	-1.63891
25	0.19166	0.07	1.6985	9.642267	1.715243	0.19197	0.0675	-1.672	9.639767	-1.65526
26	0.195362	0.0685	1.7105	9.780927	1.724498	0.19698	0.067	-1.6885	9.779427	-1.6745

Table C-1: Area and Centroid Region 1 & 2

i	a_3	x_3	y_3	x_{c3}	y_{c3}	a_4	x_4	y_4	x_{c4}	y_{c4}
1	0.06858	0.354	1.2415	10.42931	1.251926	0.082368	0.361	-1.2335	10.43631	-1.22307
2	0.076964	0.355	1.274	10.31429	1.28738	0.090896	0.374	-1.269	10.33329	-1.25562
3	0.078384	0.361	1.324	11.35145	1.333718	0.09338	0.36	-1.3145	11.35045	-1.30478
4	0.08313	0.335	1.359	10.80971	1.380464	0.099129	0.3635	-1.354	10.83821	-1.33254
5	0.094564	0.3265	1.4035	11.63893	1.427954	0.10944	0.361	-1.4015	11.67343	-1.37705
6	0.095254	0.3335	1.451	10.93079	1.481788	0.115825	0.3725	-1.4455	10.96979	-1.41471
7	0.106	0.355	1.48	11.61167	1.491183	0.117789	0.3765	-1.4795	11.63317	-1.46832
8	0.108511	0.3505	1.511	11.29427	1.510293	0.116745	0.3645	-1.514	11.30827	-1.51471
9	0.103032	0.3485	1.548	12.18517	1.581164	0.1298	0.378	-1.538	12.21467	-1.50484
10	0.110664	0.3635	1.5835	11.61057	1.587507	0.12443	0.3805	-1.5845	11.62757	-1.58049
11	0.112585	0.3365	1.636	12.59412	1.667707	0.130872	0.385	-1.639	12.64262	-1.6077

								5		9
12	0.288615	0.6505	1.6765	9.150551	1.675099	0.283276	0.6485	-1.678	9.148551	-1.6794
13	0.29469	0.6415	1.718	9.622813	1.724642	0.29887	0.6455	-1.716	9.626813	-1.70936
14	0.167634	0.4315	1.7495	11.60042	1.742306	0.17344	0.434	-1.753	11.60292	-1.76019
15	0.19602	0.47	1.7875	11.20961	1.783817	0.20648	0.478	-1.791	11.21761	-1.79468
16	0.21797	0.489	1.835	11.94214	1.733888	0.233784	0.517	-1.8355	11.97014	-1.93661
17	0.238374	0.5225	1.8835	11.09747	1.897614	0.250819	0.5385	-1.883	11.11347	-1.86889
18	0.26443	0.5565	1.924	11.01902	1.947365	0.27904	0.568	-1.919	11.03052	-1.89563
19	0.30783	0.6	1.964	10.83964	1.962885	0.304525	0.5985	-1.967	10.83814	-1.96811
20	0.338	0.635	2.004	10.72796	2.002689	0.332254	0.6245	-2.004	10.71746	-2.00531
21	0.363608	0.6615	2.033	10.693	2.043908	0.36712	0.653	-2.0285	10.6845	-2.01759
22	0.398604	0.699	2.064	10.48837	2.084895	0.41292	0.69	-2.055	10.47937	-2.0341
23	0.443497	0.7305	2.068	10.43471	2.063773	0.43036	0.717	-2.069	10.42121	-2.07323
2	0.45053	0.772	2.10	10.467	2.1145	0.4617	0.75	-	10.449	-

4	4		9	41	9	74	4	2.101	41	2.0954 1
2 5	0.48191 4	0.793	2.14 65	10.365 27	2.1632 43	0.5041 92	0.79 15	- 2.139	10.363 77	- 2.1222 6
2 6	0.49567	0.816	2.18 85	10.528 43	2.2024 98	0.5126 16	0.82 3	- 2.185	10.535 43	-2.171

Table C-2: Area and Centroid Region 3 & 4

i	a_5	x_5	y_5	x_{c5}	y_{c5}	$a_6 = a_{11}$	$x_6 = x_{11}$	$y_6 = -y_{11}$	$x_{c6} = x_{c11}$	$y_{c6} = y_{c11}$
1	0	-0.01	0	10.06531	0.010426	0.045603	-15.1109	0.987025	-5.0356	0.997451
2	0.0546	-0.01	0	9.949289	0.01338	0.046493	-15.5094	1.019621	-5.55013	1.033001
3	0	-0.01	0	10.98045	0.009718	0.047391	-15.9079	1.052217	-4.91747	1.061935
4	0.05822	-0.01	0	10.46471	0.021464	0.048296	-16.3064	1.084813	-5.83171	1.106277
5	0	-0.01	0	11.30243	0.024454	0.049208	-16.7049	1.117409	-5.3925	1.141863
6	0.06248	-0.01	0	10.58729	0.030788	0.050128	-17.1034	1.150005	-6.50614	1.180793
7	0	-0.01	0	11.24667	0.011183	0.051055	-17.5019	1.182601	-6.24527	1.193784
8	0.06556	-0.01	0	10.93377	-0.00071	0.051989	-17.9004	1.215197	-6.95666	1.21449
9	0	-0.01	0	11.82667	0.033164	0.05293	-18.2989	1.247793	-6.46227	1.280957
10	0.0686	-0.01	0	11.23707	0.004007	0.053879	-18.6974	1.280389	-7.45037	1.284396
11	0	-0.01	0	12.24762	0.031707	0.054835	-19.0959	1.312985	-6.83833	1.344692

12	0.07386	-0.01	0	8.490051	-0.0014	0.055799	-19.4944	1.345581	-10.9944	1.34418
13	0	-0.01	0	8.971313	0.006642	0.05677	-19.893	1.378177	-10.9116	1.384818
14	0.0766	-0.01	0	11.15892	-0.00719	0.057748	-20.2915	1.410773	-9.12253	1.403579
15	0.07852	-0.01	0	10.72961	-0.00368	0.058733	-20.69	1.443369	-9.95035	1.439686
16	0.08064	-0.01	0	11.44314	-0.10111	0.059726	-21.0885	1.475965	-9.63532	1.374853
17	0.08244	-0.01	0	10.56497	0.014114	0.060726	-21.487	1.508561	-10.912	1.522675
18	0.08424	-0.01	0	10.45252	0.023365	0.061733	-21.8855	1.541157	-11.4229	1.564522
19	0.08646	-0.01	0	10.22964	-0.00111	0.062748	-22.284	1.573753	-12.0443	1.572638
20	0.0883	-0.01	0	10.08296	-0.00131	0.06377	-22.6825	1.606349	-12.5895	1.605038
21	0.0898	-0.01	0	10.0215	0.010908	0.064799	-23.081	1.638945	-13.0495	1.649853
22	0.09146	-0.01	0	9.77937	0.020895	0.065836	-23.4795	1.671541	-13.6901	1.692436
23	0.09222	-0.01	0	9.694206	-0.00423	0.066879	-23.878	1.704137	-14.1738	1.69991
24	0.09298	-0.01	0	9.685412	0.00559	0.067931	-24.2765	1.736733	-14.5811	1.742323

25	0.09532	-0.01	0	9.562267	0.016743	0.068989	-24.675	1.769329	-15.1027	1.786072
26	0.09694	-0.01	0	9.702427	0.013998	0.070055	-25.0735	1.801925	-15.3611	1.815923

Table C-3: Area and Centroid Region 5, 6 & 11

i	$a_7 = a_{10}$	$x_7 = x_{10}$	$y_7 = -y_{10}$	$x_{c7} = x_{c10}$	$y_{c7} = -y_{c10}$	$(2/5)a_8 = a_9$	$x_8 = x_9$	$y_8 = y_9$	$x_{c8} = x_{c9}$	$y_{c8} = y_{c9}$
1	0.012701	-15.3647	0.962127	-5.28938	0.972552	0.031385	-15.7674	0	-5.69213	0.010426
2	0.01387	-15.7708	0.993937	-5.81152	1.007317	0.035233	-16.1742	0	-6.21495	0.01338
3	0.015045	-16.1769	1.025748	-5.18648	1.035466	0.039255	-16.581	0	-5.59058	0.009718
4	0.016229	-16.583	1.057558	-6.10833	1.079023	0.043453	-16.9878	0	-6.51312	0.021464
5	0.017419	-16.9892	1.089369	-5.67673	1.113823	0.047824	-17.3946	0	-6.0822	0.024454
6	0.018618	-17.3953	1.12118	-6.79798	1.151968	0.052371	-17.8014	0	-7.20413	0.030788
7	0.019823	-17.8014	1.15299	-6.54472	1.164173	0.057091	-18.2082	0	-6.95155	0.011183
8	0.021036	-18.2075	1.184801	-7.26374	1.184094	0.061987	-18.615	0	-7.67124	-0.00071
9	0.022257	-18.6136	1.216611	-6.77696	1.249775	0.067056	-19.0218	0	-7.18515	0.033164
10	0.023485	-19.0197	1.248422	-7.77267	1.25243	0.072301	-19.4286	0	-8.18154	0.004007
11	0.02472	-19.4259	1.280233	-7.16824	1.31194	0.07772	-19.8354	0	-7.57778	0.031707

12	0.025963	-19.832	1.312043	-11.3319	1.310642	0.083313	-20.2422	0	-11.7422	-0.0014
13	0.027214	-20.2381	1.343854	-11.2568	1.350495	0.089081	-20.649	0	-11.6677	0.006642
14	0.028471	-20.6442	1.375665	-9.47528	1.36847	0.095023	-21.0558	0	-9.88687	-0.00719
15	0.029737	-21.0503	1.407475	-10.3107	1.403792	0.10114	-21.4626	0	-10.723	-0.00368
16	0.031009	-21.4564	1.439286	-10.0033	1.338174	0.107432	-21.8694	0	-10.4162	-0.10111
17	0.03229	-21.8626	1.471096	-11.2876	1.485211	0.113897	-22.2762	0	-11.7012	0.014114
18	0.033577	-22.2687	1.502907	-11.8061	1.526272	0.120538	-22.683	0	-12.2205	0.023365
19	0.034872	-22.6748	1.534718	-12.4351	1.533603	0.127353	-23.0898	0	-12.8501	-0.00111
20	0.036175	-23.0809	1.566528	-12.9879	1.565217	0.134343	-23.4966	0	-13.4036	-0.00131
21	0.037485	-23.487	1.598339	-13.4555	1.609247	0.141507	-23.9034	0	-13.8719	0.010908
22	0.038802	-23.8931	1.630149	-14.1038	1.651045	0.148845	-24.3102	0	-14.5208	0.020895
23	0.040127	-24.2992	1.66196	-14.595	1.657733	0.156358	-24.717	0	-15.0128	-0.00423
24	0.04146	-24.7054	1.693771	-15.01	1.699361	0.164046	-25.1238	0	-15.4283	0.00559

25	0.0428	-25.1115	1.725581	-15.5392	1.742324	0.171908	-25.5305	0	-15.9583	0.016743
26	0.044147	-25.5176	1.757392	-15.8052	1.77139	0.179945	-25.9373	0	-16.2249	0.013998

Table C-4: Area and Centroid Region 7, 8, 9 & 10

i	$a_{12} = a_{13}$	$x_{12} = x_{13}$	$y_{12} = -y_{13}$	$x_{c12} = x_{c13}$	$y_{c12} = -y_{c13}$	a_{14}	x_{14}	y_{14}	x_{c14}	y_{c14}
1	0.007346	-14.5034	1.047563	-4.4281	1.057989	0.338053	-16.5989	0	-6.52359	0.010426
2	0.007253	-14.8939	1.08026	-4.93462	1.093639	0.344074	-17.0369	[illegible]	-7.07765	0.01338
3	0.007166	-15.2845	1.112956	-4.29404	1.122674	0.350111	-17.4748		-6.48439	0.009718
4	0.007083	-15.6752	1.145653	-5.20045	1.167117	0.356164	-17.9126		-7.4379	0.021464
5	0.007005	-16.0659	1.17835	-4.75347	1.202804	0.362231	-18.3503		-7.03784	0.024454
6	0.006931	-16.4567	1.211046	-5.85941	1.241835	0.368311	-18.7878		-8.19052	0.030788
7	0.006861	-16.8476	1.243743	-5.5909	1.254926	0.374403	-19.2253		-7.9686	0.011183
8	0.006794	-17.2385	1.27644	-6.29472	1.275733	0.380505	-19.6626		-8.71885	-0.00071
9	0.00673	-17.6295	1.309137	-5.7928	1.342301	0.386618	-20.0999		-8.26323	0.033164
10	0.00667	-18.0205	1.341834	-6.77343	1.345842	0.39274	-20.5371		-9.29002	0.004007
11	0.006612	-18.4116	1.374531	-6.15395	1.406238	0.39887	-20.9742		-8.71659	0.031707

12	0.006557	-18.8027	1.407228	-10.3026	1.405827	0.405008	-21.4113		-12.9112	-0.0014
13	0.006504	-19.1938	1.439925	-10.2125	1.446567	0.411154	-21.8482		-12.8669	0.006642
14	0.006454	-19.585	1.472622	-8.41611	1.465428	0.417306	-22.2852		-11.1162	-0.00719
15	0.006406	-19.9763	1.50532	-9.23666	1.501637	0.423465	-22.722		-11.9824	-0.00368
16	0.006359	-20.3675	1.538017	-8.91438	1.436905	0.42963	-23.1589		-11.7057	-0.10111
17	0.006315	-20.7588	1.570714	-10.1839	1.584828	0.4358	-23.5956		-13.0207	0.014114
18	0.006272	-21.1501	1.603411	-10.6876	1.626776	0.441975	-24.0323		-13.5698	0.023365
19	0.006231	-21.5415	1.636108	-11.3018	1.634994	0.448156	-24.469		-14.2294	-0.00111
20	0.006192	-21.9329	1.668806	-11.8399	1.667494	0.45434	-24.9057		-14.8127	-0.00131
21	0.006154	-22.3243	1.701503	-12.2928	1.712411	0.460529	-25.3423		-15.3108	0.010908
22	0.006117	-22.7157	1.7342	-12.9263	1.755096	0.466722	-25.7788		-15.9895	0.020895
23	0.006082	-23.1071	1.766898	-13.4029	1.76267	0.472919	-26.2154		-16.5111	-0.00423
24	0.006048	-23.498	1.799595	-13.8032	1.805185	0.47912	-26.651		-16.956	0.00559

		6					8		4	
25	0.006016	-23.8901	1.832292	-14.3178	1.849035	0.485323	-27.0883		-17.516	0.016743
26	0.005984	-24.2816	1.86499	-14.5692	1.878987	0.49153	-27.5247		-17.8123	0.013998

Table C-5: Area and Centroid Region 12, 13 & 14

Appendix D: Excel Programming Lines and Keys

$\acute{X}$ **for Region 12 and 13:**

(1/(2*A))*(((16/5)*(L^2)*(y^5)/(T3^4))- ((8/3)*(L^2)*(y^3)/(T3^2))+ ((L^2)*(y)))

(1/(2*D73))*(((16/5)*(D72^2)*(y^5)/(D19^4))- ((8/3)*(D72^2)*(y^3)/(D19^2))+ ((D72^2)*(y)))

f(y) = ((1/(2*D73))*(((16/5)*(D72^2)*((D19/2)^5)/(D19^4))- ((8/3)*(D72^2)*((D19/2)^3)/(D19^2))+ ((D72^2)*((D19/2)))))-((1/ (2*D73))*(((16/5)*(D72^2)*(((D19/2)-0.04)^5)/(D19^4))- ((8/3)*(D72^2)*(((D19/2)- 0.04)^3)/(D19^2))+ ((D72^2)*(((D19/2)-0.04)))))

a = ((16/5)*(L^2)*(y^5)/(T3^4))

b = ((8/3)*(L^2)*(y^3)/(T3^2))

c = ((L^2)*(y))

$\acute{Y}$ **for Region 12 and 13:**

(1/A)*((-L)*(y^4)/(T3^2)+ (0.5*L*(y^2)))

(1/D73)*((-D72)*(y^4)/(D19^2)+ (0.5*D72*(y^2)))

f (y) = ((1/D73)*((-D72)*((D19/2)^4)/(D19^2)+ (0.5*D72*((D19/2)^2))))- ((1/D73)*((-D72)*(((D19/2)-0.04)^4)/(D19^2)+ (0.5*D72*(((D19/2)-0.04)^2))))

a = (-L)*(y^4)/(T3^2)

b = (0.5*L*(y^2))

$\acute{X}$ **for Region 14:**

(1/(2*A))*(((16/5)*(L^2)*(y^5)/(T3^4))- ((8/3)*(L^2)*(y^3)/(T3^2))+ ((L^2)*(y)))

-(1/(2*A))*(((16/5)*((L-tg)^2)*(y^5)/((T3-(2*tg))^4))- ((8/3)*((L-tg)^2)*(y^3)/((T3-(2*tg))^2))+ (((L-tg)^2)*(y)))

(1/(2*(D74-D75)))*(((16/5)*(D72^2)*(y^5)/(D19^4))- ((8/3)*(D72^2)*(y^3)/(D19^2))+ ((D72^2)*(y)))

-(1/(2*(D74-D75)))*(((16/5)*((D72-0.04)^2)*(y^5)/((D19-(2*0.04))^4))- ((8/3)*((D72-0.04)^2)*(y^3)/((D19-(2*0.04))^2))+ (((D72-0.04)^2)*(y)))

f (y) =

((1/(2*(D74-D75)))*(((16/5)*(D72^2)*(((D19/2)-0.04)^5)/(D19^4))- ((8/3)*(D72^2)*(((D19/2)-0.04)^3)/(D19^2))+ ((D72^2)*(((D19/2)-0.04))))-(1/(2*(D74-D75)))*(((16/5)*((D72-0.04)^2)*(((D19/2)-0.04)^5)/((D19-(2*0.04))^4))- ((8/3)*((D72-0.04)^2)*(((D19/2)-0.04)^3)/((D19-(2*0.04))^2))+ (((D72-0.04)^2)*(((D19/2)-0.04)))))-((1/(2*(D74-D75)))*(((16/5)*(D72^2)*((-((D19/2)-0.04))^5)/(D19^4))- ((8/3)*(D72^2)*((-((D19/2)-0.04))^3)/(D19^2))+ ((D72^2)*((-((D19/2)-0.04)))))-(1/(2*(D74-D75)))*(((16/5)*((D72-0.04)^2)*((-((D19/2)-0.04))^5)/((D19-(2*0.04))^4))- ((8/3)*((D72-0.04)^2)*((-((D19/2)-0.04))^3)/((D19-(2*0.04))^2))+ (((D72-0.04)^2)*((-((D19/2)-0.04))))))

Total $\acute{X}$

=((D20*D21)+(D25*D26)+(D30*D31)+(D35*D36)+(D40*D41)+(2*D57*D58)+(2*D62*D63)+(D67*D68)+(2*D73*D79)+((D74-D75)*D84)+(D92*D93*2)+(D92*D97*2)+(D92*D101*2) +(D107*D108)+(D113*D114))/(D20+D25+D30+D35+D40+(2*D57)+(2*D62)+D67+(2*D73)+(D74-D75)+(D92*6)+D107+D113)

Total $\acute{Y}$

=((D20*D22)+(D25*D27)+(D30*D32)+(D35*D37)+(D57*D59)+(-D57*D59)+(D62*D64)+(-D62*D64)+(D73*D80)+(-D73*D80)+(D107*D109)+(D113*D115))/(D20+D25+D30+D35+D40+(2*D57)+(2*D62)+D67+(2*D73)+(D74-D75)+(D92*6)+D107+D113)

Total Inertia I_X

=(D20*(D24^2))+(D25*(D29*2))+(D30*(D34^2))+(D35*(D39^2))+(D40*(D44^2))*(2*D57*(D61^2))+(2*D62*(D66^2))+(D67*(D71^2))+(2*D73*(D82^2))+((D74-D75)*(D87^2))+(2*D92*(D96^2))+(2*D92*(D100^2))+(2*D92*(D104^2))+(D107*(D111^2))+(D113*(D117^2))

Total Inertia I_Y

=(D20*(D23^2))+(D25*(D28^2))+(D30*(D33^2))+(D35*(D38^2))+(D40*(D43^2))+(2*D57*(D60^2))+(2*D62*(D65^2))+(D67*(D70^2))+(2*D73*(D81^2))+((D74-D75)*(D86^2))+(2*D92*(D95^2))+(2*D92*(D99^2))+(2*D92*(D103^2))+(D107*(D110^2))+(D113*(D116^2))

APPENDIX E: CAD OF LOADING DEVICE

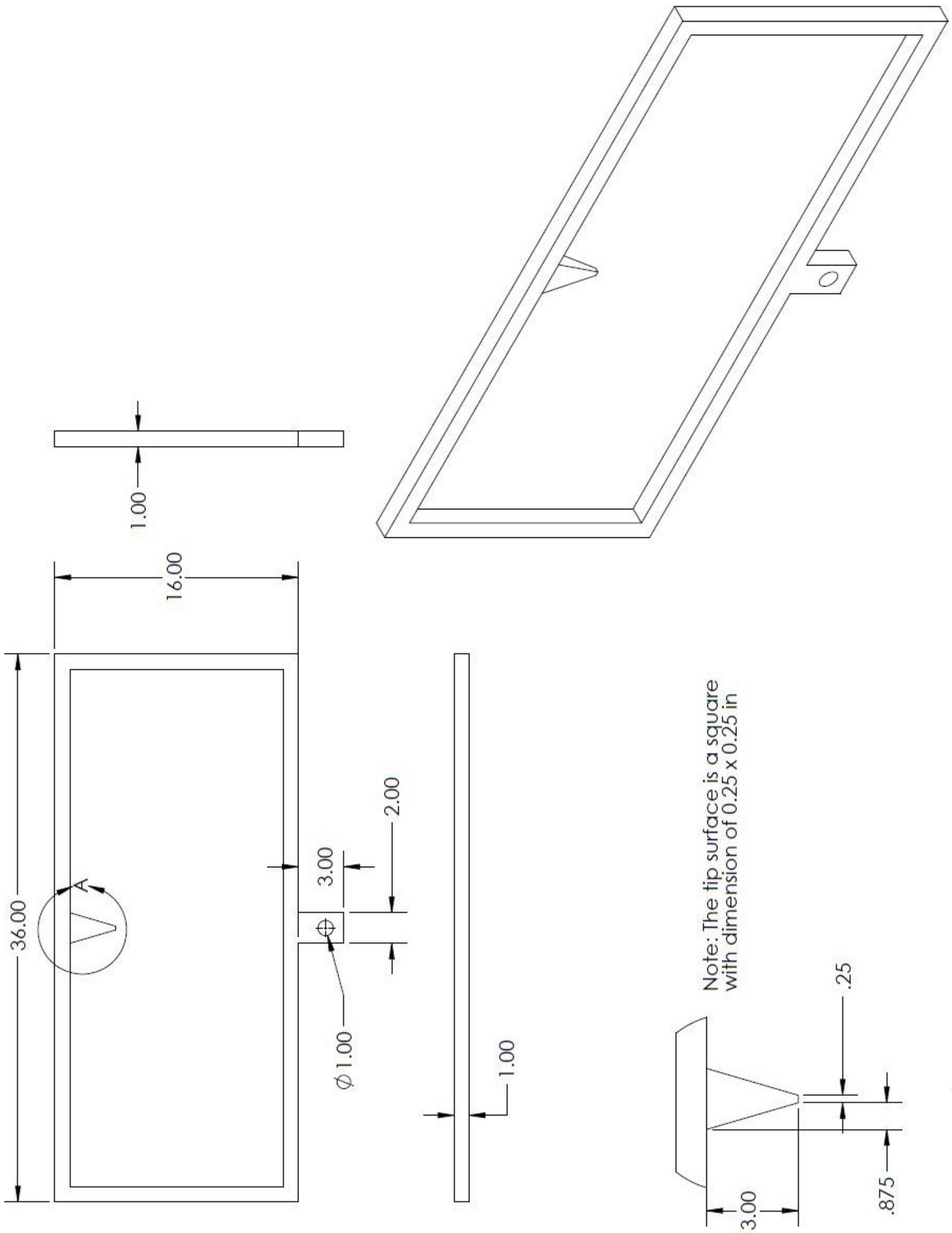

36.00
16.00
1.00
A
2.00
3.00
Ø1.00
1.00
Note: The tip surface is a square with dimension of 0.25 x 0.25 in
.25
.875
3.00